Support for Starfire Optical Range

February 1999

Prepared by:

Schafer Corporation
2000 Randolph Rd. S. E.
Suite 205
Albuquerque, NM 87106

Task Report - Naval Research Laboratory
Contract N00014-97-D-2014/001

SCHAFER CORPORATION

Submitted to *Applied Optics* 9/30/98 – Please do not cite or distribute

Modeling the Combined Effect of Static and Varying Phase Distortions on the Performance of Adaptive Optical Systems

Brent L. Ellerbroek

Starfire Optical Range, Directed Energy Directorate,
US Air Force Research Laboratory, Kirtland AFB, New Mexico 87117

David W. Tyler

Albuquerque High Performance Computing Center, University of New Mexico,
Albuquerque, New Mexico 87131

Abstract

The end-to-end performance achieved by an adaptive optical (AO) imaging system is determined by a combination of the residual time-varying phase distortions associated with atmospheric turbulence, and the quasi-static unsensed and uncorrectable aberrations in the optical system itself. Although the effects of these two errors on the time averaged Strehl ratio and the time averaged optical transfer function (OTF) of the AO system are not formally separable, such an approximation is found to be accurate to within a few per cent for a range of representative residual wave-front errors. In these calculations, we have combined static optical system aberrations and time-varying residual phase distortion characteristic of deformable mirror (DM) fitting error, wave-front sensor (WFS) noise, and anisoplanatism. The static aberrations consist of focus errors of varying magnitudes as well as a combination of unsensed and uncorrectable mirror figure errors derived from modeling by the Gemini 8-meter Telescopes project. The overall Strehl ratios and OTF's due to the combined effect of these error sources are well approximated as products of separate factors for the static and time-varying aberrations, as long as the overall Strehl ratio due to both errors is greater than about 0.1. For lower Strehl ratios the products provide lower bounds on the actual values of the Strehl ratio and OTF. The speckle transfer function (STF) is also well approximated by a product of two functions, but only where AO compensation is sufficiently good that speckle imaging techniques are usually not required.

OCIS codes: 010.1080, 010.4850, 100.1830, 110.6150, 110.6770

1. Introduction

The existing literature suggests that most adaptive optics (AO) performance analysis for large, ground based telescopes is partitioned into separate treatments of the phase distortions, or aberrations, introduced by atmospheric turbulence, and aberrations introduced by

the telescope optics themselves.[1,2] Although much expense and modeling effort is applied to characterize these two wave-front error sources separately, overall optical system performance is frequently estimated by simply multiplying the corresponding Strehl ratios. For AO-compensated wave-fronts with residual errors, this multiplicative approximation is not formally exact; since the costs and performance specifications associated with large telescopes are so challenging, it may be prudent to model the interaction of turbulence-induced phase distortions and telescope aberrations with greater precision. This paper summarizes the results of such a study. For a range of representative atmospheric phase distortions partially compensated by adaptive optics and several sample telescope aberrations, the multiplicative estimate of the overall system Strehl ratio is a remarkably good approximation as long as this quantity is larger than about 0.1. At somewhat lower performance levels the multiplicative approximation can be used as a moderately conservative lower bound on the actual Strehl ratio. Similar conclusions apply to approximating an "end-to-end" optical transfer function (OTF) which accounts for all of the wave-front errors in the system as a product of two terms computed separately for the effects of the atmospheric turbulence and the telescope optics. For higher-order moments of the OTF such as the speckle transfer function (STF) the multiplicative approximation begins to fail at a somewhat higher Strehl ratio, but reasonable accuracy can still be achieved at Strehl ratios of about 0.3 if the residual wave-front aberrations are distributed over a range of spatial frequencies.

The validity of these approximations simplifies the design and use of AO systems for large telescopes in several ways. During system design an overall system OTF specification may be factored into two allocations for the telescope optics and the AO system which may be addressed separately. When AO-compensated imagery is to be postprocessed using deconvolution of the OTF, the end-to-end system OTF can be approximated as a product of (a) the atmospheric OTF as estimated from closed-loop wave-front sensor (WFS) data[3] and (b) the optical system OTF as calibrated using a local reference source. If speckle imaging techniques[4] are used, the system STF can also be approximated by the product of an atmospheric STF (estimated from WFS data) and an optical system STF.

The phase-only Fourier optics model used for this study is described in section 2. The end-to-end optical system OTF is proportional to the autocorrelation of the complex-valued function U, the optical field obtained in the exit pupil of the telescope from a monochromatic point source after propagation through the atmosphere, the AO system, and the telescope optics. The pupil function U can be divided into three parts: The real-valued transmittance function of the optical system, the static telescope aberrations ϕ_s which are unsensed or uncorrected by the adaptive optics, and the time-varying residual atmospheric distortions ϕ_v left uncompensated by the AO system. The time-averaged OTF of the system is obtained by averaging over the statistics of the atmospheric phase profile ϕ_v, which is assumed to be a zero-mean, normally distributed random variable. The time averaged Strehl ratio S can be computed as the integral of the OTF. Without adaptive optics, the stationarity of turbulence-induced phase distortions allows the OTF to be written as a product of two terms which depend separately upon ϕ_s and the statistics of ϕ_v. For atmospheric turbulence which has been partially compensated by AO stationarity may not be assumed, however, and such a decoupling is not mathematically valid. Experience and intuition still suggest that for small phase errors the combined effect of ϕ_v and ϕ_s should be well approximated by the product of separately computed transfer functions or Strehl ratios. For speckle imaging,

however, the form of the STF casts doubt on the validity of a product approximation for the end-to-end transfer function even without AO compensation.

Sample results quantifying the accuracy of these approximations are summarized in section 3 for a range of representative telescope optical aberrations and residual turbulence-induced phase errors. Three varieties of residual turbulence-induced errors driven primarily by deformable mirror (DM) fitting error, wave-front sensor (WFS) noise, and anisoplanatism are combined with three different magnitudes of a static focus error for a sample Shack-Hartmann-based AO system with 8×8 WFS subapertures and 9×9 DM actuators. Two more specific cases are also considered using atmospheric, AO, and aberration parameters corresponding to the Gemini-North 8-meter telescope.[5,6] The results of these calculations form the basis for the conclusions given in the first paragraph above.

Section 4 presents sample sky coverage results obtained using the Gemini telescope OTF's as computed in section 3. Here "sky coverage" is defined as the function $P(S \geq S_0)$, the fraction of a specified region of the sky for which the telescope and AO system achieve an end-to-end performance level S at least equal to a desired threshold S_0.[7,8,6,9] Sample performance metrics for sky coverage include time average Strehl ratio and the coupling efficiency for feeding an optical fiber or spectrometer slit. This function is determined by a combination of guide star, atmospheric, science instrument, AO system, and telescope parameters, including the unsensed and uncorrectable aberrations in the telescope optics. For sample Gemini-North parameters we find that the reduction in sky coverage due to telescope aberrations for a specific instrument, such as a spectrometer, can depend upon the shape of the aberrated point spread function (PSF) as well as upon its Strehl ratio. In this case the end-to-end OTF of the AO system, accounting for both atmospheric and telescope error sources, must be used to compute accurate sky coverage estimates. Sky coverage estimates derived by simpler scaling laws can be significantly pessimistic.

Finally, section 5 is a brief summary of the principal results of the paper.

2. Analysis Summary

Using Fourier optics methods,[10,11] the monochomatic, incoherent, isoplanatic imaging performance of an optical system can be modeled as a spatial filtering operation by the transfer function $\mathrm{OTF}(\boldsymbol{\kappa})$. This tranfer function is described by the equation

$$\mathrm{OTF}(\boldsymbol{\kappa}) = \frac{\int d\boldsymbol{r}\, U(\boldsymbol{r}) U^*(\boldsymbol{r} - \lambda\boldsymbol{\kappa})}{\int d\boldsymbol{r}\, |U(\boldsymbol{r})|^2}, \tag{2.1}$$

Where κ is a two-dimensional spatial frequency variable, λ is the wavelength of the light, the integration variable $\boldsymbol{r}$ denotes coordinates in the telescope exit pupil, and the function U is the optical field obtained in the exit pupil when imaging a point source. If atmospheric scintillation is neglected, the field U is related to the residual turbulence-induced phase distortion ϕ_v left uncorrected by the AO system by the formula

$$U(\boldsymbol{r}) = P(\boldsymbol{r}) \exp\left[i\phi_v(\boldsymbol{r})\right], \tag{2.2}$$

where P is the field in the exit pupil with no atmospheric turbulence. The notation "ϕ_v" has been selected to suggest that the residual turbulence-induced phase distortion is a time-varying quantity, and this function is assumed to be a zero-mean, normally distributed

random variable. The turbulence-free field P is referred to as the generalized pupil function of the telescope and may be written in the form

$$P(\boldsymbol{r}) = P_0(\boldsymbol{r}) \exp\left[i\phi_s(\boldsymbol{r})\right], \tag{2.3}$$

where P_0 is a real-valued optical transmittance function and ϕ_s is the static or quasi-static wave-front error due to uncorrectable or unsensed aberrations in the telescope optics. Examples of such errors include errors at unobservably high spatial frequencies on the primary mirror, and aberrations in optical elements within instruments which are not included in the WFS optical path. Substituting Eq.'s (2.2) and (2.3) back into Eq. (2.1) yields the relationship

$$\mathrm{OTF}(\boldsymbol{\kappa}) = \frac{\int d\boldsymbol{r}\, P_0(\boldsymbol{r}) P_0(\boldsymbol{r} - \lambda\boldsymbol{\kappa}) \exp\left\{i\left[\phi_s(\boldsymbol{r}) - \phi_s(\boldsymbol{r} - \lambda\boldsymbol{\kappa})\right]\right\} \exp\left\{i\left[\phi_v(\boldsymbol{r}) - \phi_v(\boldsymbol{r} - \lambda\boldsymbol{\kappa})\right]\right\}}{\int d\boldsymbol{r}\, P_0^2(\boldsymbol{r})}, \tag{2.4}$$

between the optical system OTF and the wave-front aberrations ϕ_s and ϕ_v induced by the telescope optics and uncompensated atmospheric turbulence.

For long exposure imaging it is the time averaged value $\langle \mathrm{OTF}(\boldsymbol{\kappa}) \rangle$ which is of interest, where the notation $\langle \cdots \rangle$ denotes ensemble averaging over the statistics of atmospheric turbulence and WFS measurement noise. Since the telescope aberration function ϕ_s is assumed to be static, only the final term in the numerator of Eq. (2.4) is a random quantity. Because the uncorrected turbulence-induced aberration ϕ_v is modeled as a zero-mean, normally distributed random variable, the expected value of this term takes the form

$$\begin{aligned} \left\langle \exp\left\{i\left[\phi_v(\boldsymbol{r}) - \phi_v(\boldsymbol{r} - \lambda\boldsymbol{\kappa})\right]\right\} \right\rangle &= \exp\left\{-\tfrac{1}{2}\left\langle \left[\phi_v(\boldsymbol{r}) - \phi_v(\boldsymbol{r} - \lambda\boldsymbol{\kappa})\right]^2 \right\rangle\right\} \\ &= \exp\left[-\tfrac{1}{2}\mathcal{D}(\boldsymbol{r}, \boldsymbol{r} - \lambda\boldsymbol{\kappa})\right], \end{aligned} \tag{2.5}$$

where $\mathcal{D}(\boldsymbol{r}, \boldsymbol{r} - \lambda\boldsymbol{\kappa}) = \left\langle \left[\phi_v(\boldsymbol{r}) - \phi_v(\boldsymbol{r} - \lambda\boldsymbol{\kappa})\right]^2 \right\rangle$ is the structure function of the residual turbulence-induced phase error ϕ_v. The time averaged OTF of the optical system is therefore given by the expression

$$\langle \mathrm{OTF}(\boldsymbol{\kappa}) \rangle = \frac{\int d\boldsymbol{r}\, P_0(\boldsymbol{r}) P_0(\boldsymbol{r} - \lambda\boldsymbol{\kappa}) \exp\left\{i\left[\phi_s(\boldsymbol{r}) - \phi_s(\boldsymbol{r} - \lambda\boldsymbol{\kappa})\right]\right\} \exp\left[-\tfrac{1}{2}\mathcal{D}(\boldsymbol{r}, \boldsymbol{r} - \lambda\boldsymbol{\kappa})\right]}{\int d\boldsymbol{r}\, P_0^2(\boldsymbol{r})}. \tag{2.6}$$

The point spread function (PSF) of the optical system and related quantities can be now evaluated in terms of the time averaged OTF. In particular, the time averaged Strehl ratio S of the optical system can be computed using the formula

$$S = \int d\boldsymbol{\kappa}\, \langle \mathrm{OTF}(\boldsymbol{\kappa}) \rangle. \tag{2.7}$$

From the last two equations it is clear that the time averaged OTF and the Strehl ratio S are functions of the static telescope aberration ϕ_s and $\mathcal{D}$, the structure function of the time-varying phase errors ϕ_v. It is convenient to abbreviate this relationship using the notation $\langle \mathrm{OTF}(\kappa) \rangle_{(\phi_s, \mathcal{D})}$ and $S_{(\phi_s, \mathcal{D})}$. For general values of ϕ_s and $\mathcal{D}$ the dependance of

the OTF and the Strehl ratio upon these quantities is nonseparable, except in the special case where either the static phase difference $\phi_s(\boldsymbol{r}) - \phi_s(\boldsymbol{r} - \lambda\boldsymbol{\kappa})$ or the structure function $\mathcal{D}(\boldsymbol{r}, \boldsymbol{r} - \lambda\boldsymbol{\kappa})$ is actually a function of $\lambda\boldsymbol{\kappa}$ alone. This is indeed the case for stationary models of uncompensated atmospheric turbulence, but these conditions do not generally hold for the residual wave-front errors left uncorrected by an AO system. Experience and intuition suggest, however, that multiplicative approximation

$$\langle \mathrm{OTF}(\boldsymbol{\kappa}) \rangle_{(\phi_s, \mathcal{D})} \approx \langle \mathrm{OTF}(\boldsymbol{\kappa}) \rangle_{(0, \mathcal{D})} \left[\frac{\langle \mathrm{OTF}(\boldsymbol{\kappa}) \rangle_{(\phi_s, 0)}}{\langle \mathrm{OTF}(\boldsymbol{\kappa}) \rangle_{(0,0)}} \right], \tag{2.8}$$

should still be reasonably accurate as long as the quantities ϕ_s and $\mathcal{D}$ are not too large.

For the Strehl ratio S, the corresponding multiplicative approximation can be justified for two types of phase errors. First, AO systems operating under benign conditions will leave small residual phase errors. For this case we may use[12]

$$S \approx 1 - \sigma^2, \tag{2.9}$$

where σ^2 is the variance of ϕ over the telescope aperture. While this approximation would not be accurate for uncompensated turbulence,[13] the assumption of small residual phase errors justifies its use in this case. Substituting $\phi = \phi_v + \phi_s$ into Eq. (2.9) and assuming that the two terms are spatially uncorrelated yields

$$\begin{aligned} S_{(\phi_s, \mathcal{D})} &\approx 1 - \left(\sigma_v^2 + \sigma_f^2\right) \\ &\approx \exp\left[-(\sigma_v^2 + \sigma_f^2)\right] \\ &\approx S_{(0, \mathcal{D})} S_{(\phi_s, 0)}, \end{aligned} \tag{2.10}$$

where σ_v^2 and σ_s^2 denote the variances of the two terms of the wave-front error. For sufficiently small total phase, then, the overall Strehl ratio may be approximated by the product of two independent terms, regardless of the spatial distribution of the phase errors. Secondly, consider the limit case of residual turbulence-induced phase errors which are spatially white, so that $\mathcal{D}(\boldsymbol{r}, \boldsymbol{r} - \lambda\boldsymbol{\kappa}) \equiv 2\sigma_v^2$ for all $\boldsymbol{r}$ and all nonzero $\boldsymbol{\kappa}$. Combining this assumption with Eq.'s (2.6) and (2.7) yields

$$\begin{aligned} S &= \int d\boldsymbol{\kappa} \, \langle \mathrm{OTF}(\boldsymbol{\kappa}) \rangle \\ &= \exp(-\sigma_v^2) \frac{\int d\boldsymbol{r} \, P_0(\boldsymbol{r}) P_0(\boldsymbol{r} - \lambda\boldsymbol{\kappa}) \exp\left\{ i \left[\phi_s(\boldsymbol{r}) - \phi_s(\boldsymbol{r} - \lambda\boldsymbol{\kappa}) \right] \right\}}{\int d\boldsymbol{r} \, P_0^2(\boldsymbol{r})} \\ &= S_{(0, \mathcal{D})} S_{(\phi_s, 0)}. \end{aligned} \tag{2.11}$$

so that the overall Strehl is again given as the product of two terms. As shown by the results presented in Section 3 below, one of these two assumptions on the distribution of σ_v will generally be valid for an AO system providing any useful degree of atmospheric turbulence compensation.

Finally, for some applications higher moments of the OTF may be of interest as well. Low-order AO systems designed to compensate turbulence with very dim guide star references can fail, in severe seeing conditions, to provide PSFs in the so-called "sharp core"

regime, where there is a reasonable fraction of the total PSF intensity in a stable diffraction-limited central core. If conditions are poor enough, speckle imaging techniques[14] can be required to achieve reasonable stability in the post-processed image.[4] While many deconvolution methods require only an estimate of the long-exposure OTF, speckle imaging without observation of a calibration star would require WFS estimates of higher moments of the atmospheric OTF, such as the speckle transfer function (STF), cross-spectrum, and bispectrum. For this reason, we also consider approximation of the STF by the product of the atmospheric STF and the optical system STF. Under the same conditions used to develop the OTF, the STF is given by

$$\begin{aligned}\mathrm{STF}(\boldsymbol{\kappa}) &= \left\langle |\mathrm{OTF}(\boldsymbol{\kappa})|^2 \right\rangle \\ &= \int d\boldsymbol{r} \int d\boldsymbol{r}'\, P_0(\boldsymbol{r}) P_0(\boldsymbol{r}-\lambda\boldsymbol{\kappa}) P_0(\boldsymbol{r}') P_0(\boldsymbol{r}'-\lambda\boldsymbol{\kappa}) \\ &\quad \times \exp\{-i[\phi_s(\boldsymbol{r}) - \phi_s(\boldsymbol{r}-\lambda\boldsymbol{\kappa}) - \phi_s(\boldsymbol{r}') + \phi_s(\boldsymbol{r}'-\lambda\boldsymbol{\kappa})]\} \\ &\quad \times \langle \exp\{-i[\phi_v(\boldsymbol{r}) - \phi_v(\boldsymbol{r}-\lambda\boldsymbol{\kappa}) - \phi_v(\boldsymbol{r}') + \phi_v(\boldsymbol{r}'-\lambda\boldsymbol{\kappa})]\}\rangle \,. \end{aligned} \tag{2.12}$$

Because the expectation is over phase factors which are functions of both variables of integration, it is not stationary and can not be factored outside the integrals. If AO compensation is good, the residual atmospheric phase ϕ_v will be small, but in this case the resulting images are in the sharp core regime where we assume speckle processing would not be used. To see whether a larger domain exists over which the STF may be approximated as a product of factors, we will consider the approximation

$$\mathrm{STF}(\boldsymbol{\kappa})_{(\phi_s,\mathcal{D})} \approx \mathrm{STF}(\boldsymbol{\kappa})_{(0,\mathcal{D})} \left[\frac{\mathrm{STF}(\boldsymbol{\kappa})_{(\phi_s,0)}}{\mathrm{STF}(\boldsymbol{\kappa})_{(0,0)}}\right]. \tag{2.13}$$

The extent to which the above multiplicative approximations apply for a range of representative AO imaging scenarios is explored in the following section.

3. Sample Numerical Results

A. Cases Considered

The formulas developed in the preceeding section have been applied to study the interaction of turbulence-induced phase errors with unsensed and uncorrectable static telescope aberrations for a number of sample AO imaging scenarios. The four cases considered are summarized in Table 1. The first three cases relate to a generic Shack-Hartmann-based AO system with 8×8 WFS subapertures and 9×9 DM actuators, with residual turbulence-induced phase errors driven by DM fitting error, WFS noise, and anisoplanatism. The techniques used to evaluate the structure function $\mathcal{D}$ of the residual turbulence-induced phase distortions for each of these cases have been described elsewhere.[15] The static telescope aberration is a simple focus error for all three of these cases; in practice such an error could result from either an optical misalignment or by miscalculating the effective range of a laser guide star.

The last of the four cases is based upon atmospheric, AO, and telescope parameters derived from design studies for the Gemini-North 8-meter telescope.[5,6] Here the turbulence-induced residual phase errors are primarily a combination of fitting error and focus anisoplanatism for a laser guide star generated in the mesospheric sodium layer. An estimate of typical unsensed and uncorrectable optical aberrations for Gemini-North is illustrated in Fig. 1. Uncorrectable mirror polishing and mounting errors have been studied in great detail for Gemini, while the noncommon path errors between the WFS and science instrument optics remain budgeted allocations at this time. The phase profile in Fig. 1 is a sum of measured primary mirror mounting and polishing errors, a very small simulated mounting error for the secondary mirror, and a "typical" noncommon path error represented as a sum of low-order Zernike modes. This phase profile yields a combined telescope and instrument Strehl ratios of about 0.70 at a wavelength of $1.65\,\mu$m , and a more benign case with a Strehl ratio of about 0.85 has also been considered. These two values correspond roughly to the Gemini specification for the noncommon path errors and the smallest errors which can realistically be expected.

B. Parametric Results

Fig. 2 illustrates the Strehl ratios computed for the first three cases described in Table 1. The solid curves for the "exact Strehl ratio" have been computed using Eq. (2.7), and the dashed curves for the "multiplicative approximation" are based upon Eq. (2.10). Results for DM fitting error combined with varying amounts of static focus error are summarized in Fig. 2a for subaperture widths equal to 1, 2, and 4 times the turbulence-induced effective coherence diameter r_0, and static focus errors with values between 0 and 1 radian RMS. The multiplicative approximation to the overall Strehl ratio has a worst-case relative error of no more than about six per cent, even for overall Strehl ratios as low as two per cent. In this last case the approximation is accurate even with relatively large residual phase distortions because the errors are high spatial frequency and approximately white.

Analogous Strehl ratio results for varying amounts of random phase errors due to WFS noise and anisoplanatism are plotted in Fig.'s 2b and 2c. Here the relative errors in the multiplicative approximation remain below about five per cent for Strehl ratios no lower than 0.2, and no more than about ten per cent for Strehl ratios on the order of 0.1. These somewhat larger errors in the approximation occur because the random phase errors due to WFS noise and anisoplanatism contain nonnegligible low spatial frequency modes, which do not necessarily have equal power everywhere in the pupil.

Results on the accuracy of the multiplicative approximation for the end-to-end optical system OTF due to combinations of the errors considered above are summarized in Fig.'s 3 and 4. The curves labeled "exact OTF" and "transfer function approximation" have been computed using Eq.'s (2.6) and (2.8), respectively. These plots are for the case of a static focus error of 0.7 radians RMS, which corresponds to a Strehl ratio of about 0.6 without atmospheric turbulence. As illustrated in Fig. 3, this aberration reduces the OTF to about 45 per cent of its diffraction limited value at a normalized spatial frequency of one-half the diffraction-limited cutoff frequency. The OTF's computed for a combination of DM fitting error and this static focus error are plotted in Fig. 4a. The agreement between the actual OTF and the multiplicative approximation is excellent, once again because the DM fitting

error has so little low spatial frequency content. OTF values for wave-front errors induced by WFS noise or anisoplanatism are summarized in Fig.'s 4b and 4c. Here the worst case relative error between the actual OTF and the multiplicative approximation is on the order of 12 to 18 per cent for cases where the overall end-to-end Strehl ratio is from 6 to 20 per cent, and about five percent for cases where the end-to-end Strehl ratio is from 20 to 30 per cent. This level of agreement should be adequate for developing system performance specifications and many image postprocessing applications.

Fig. 5 shows STF's for subaperture widths as in Fig.'s 2a and 4a; $d = 1$, 2, and 4 times r_0. The solid curves plot the exact results computed using Eq. (2.12), and the dashed curves indicate the multiplicative approximation given by Eq. (2.13). Fig. 5a plots exact and approximate STF's for a static focus error of 0.2 radians RMS. For this small focus error, the exact STF is very well approximated by the product formula given by Eq. (2.13), with the approximations being numerically indistinguishable from the exact STF's for $d/r_0 = 1$ and 2. In Fig. 5b, the same plots are shown for a static focus error of 0.7 radians RMS. Here, the exact STF's are again well approximated for $d/r_0 = 1$ and 2 with a maximum relative error of about 15 percent at a frequency of 0.6. For $d/r_0 = 4$, however, the maximum relative error is about 80 per cent. In Fig. 5c, finally, the static focus error has been increased to 1 radian RMS. and the approximation is no longer very useful. For this case, the relative error is about 40 percent at midband for $d/r_0 = 1$ and over 75 percent for $d/r_0 = 2$. For $d/r_0 = 4$. the approximation fails rather spectacularly beyond a spatial frequency of about 0.3. Unfortunately, accurate estimates of the STF are likely to be most useful exactly when d/r_0 is large.

The corresponding STF results for residual phase errors due to anisoplanatism are illustrated in Fig.'s 6 and 7. In Fig. 6 the static focus error is 0.7 radians RMS, and the atmospheric phase residuals are provided by angular offsets between the science object and guidestar of 0.5. 1, and 2 times the isplanatic angle θ_0. For $\theta/\theta_0 = 0.5$, Eq. (2.13) provides a good approximation to $\mathrm{STF}(\boldsymbol{\kappa})_{(\phi_s,\mathcal{D})}$. In Fig. 7a, we show $\mathrm{STF}(\boldsymbol{\kappa})_{(0,0)}$ and $\mathrm{STF}(\boldsymbol{\kappa})_{(\phi_s,\mathcal{D})}$, along with the individual factors $\mathrm{STF}(\boldsymbol{\kappa})_{(0,\mathcal{D})}$ and $\mathrm{STF}(\boldsymbol{\kappa})_{(\phi_s,0)}$ and the approximation Eq. (2.13). Although $\mathrm{STF}(\boldsymbol{\kappa})_{(0,\mathcal{D})}/\mathrm{STF}(\boldsymbol{\kappa})_{(0,0)} \approx 0.5$ at midband, the maximum relative STF error using Eq. (2.13) is still only 19 percent. For the case of $\theta/\theta_0 = 2$ illustrated in Fig. 7b. however, Eq. (2.13) begins to be unreliable. The STF attenuation due to atmospheric and static sources are roughly equal, with $\mathrm{STF}(\boldsymbol{\kappa})_{(\phi_s,0)} = 0.18 \times \mathrm{STF}(\boldsymbol{\kappa})_{(0,0)}$ and $\mathrm{STF}(\boldsymbol{\kappa})_{(0,\mathcal{D})} = 0.2 \times \mathrm{STF}(\boldsymbol{\kappa})_{(0,0)}$ at midband. These conditions lead to a relative STF error of 60 percent.

C. Gemini Results

The results obtained with the Gemini-North telescope and AO parameters listed in the final column of Table 1 are summarized in Table 2, Fig. 8, and Fig. 9. The formulas from section 2 used for these calculations are as listed in subsection 3 B above. Table 2 list Strehl ratios at wavelengths of 1.20, 1.65, and 2.20 μm computed for residual phase errors due to atmospheric turbulence alone, optical aberrations alone, and a combination of the two error sources. The relative error in the multiplicative approximation to the overall Strehl ratio is no larger than about four per cent over this range of cases. One-dimensional slices through the corresponding OTF's for the 1.65 μm case are plotted in Fig. 9. Once again, there is very

good agreement between the exact calculation of the end-to-end OTF and a multiplicative approximation using two separate transfer functions.

In Fig. 9 we plot the various STF's for the "typical" Gemini aberrations and nominal atmospheric phase distortions at a wavelength of 1.2 μm. The RMS phase is 0.62 radians for the static aberrations and 0.47 radians for the atmospheric residual. Because the Gemini errors are not azimuthally symmetric, like focus, the curves shown are radial averages of two dimensional STF's. With a total Strehl ratio of about 0.3, the resulting PSF is within the "sharp core" regime, and in practice speckle imaging methods would probably not be required. Still, we point out that since the STF attenuation due to static aberrations is fairly evenly distributed over a range of frequencies, a relative error of about 8 percent is achieved at midband using Eq. (2.13). This level of agreement is obtained for a static aberration with a RMS value approximately equal to the fixed focus error considered in Fig. 6b, for which the accuracy of the multiplicative approximation was much poorer. In comparison with the OTF results presented in Fig.'s 4 and 8, it appears that the accuracy of Eq. (2.13) for the STF depends more strongly upon the specific nature of the static aberrations.

4. Sky Coverage Calculations

The so-called "sky coverage" of an AO system for an astronomical telescope can be expressed in terms of the function $P(S \geq S_0)$, the fraction of a specified region of the sky for which the system achieves an end-to-end performance level S at least equal to a desired threshold S_0.[7] Sky coverage can be computed for a variety of performance metrics, such as time averaged Strehl ratio or the slit power coupling for a spectrometer.[6,16] This function is determined by a combination of guide star, atmospheric, science instrument, AO system, and telescope parameters, including the unsensed and uncorrectable aberrations in the telescope optics. Sky coverage remains an issue for laser guide star (LGS) AO systems, since a natural guide star (NGS) is still required to measure the full aperture tip and tilt of the wave-front. An LGS AO system will consequently obtain best results for science objects very near to a bright NGS, while performance for other objects will be degraded by tip/tilt jitter arising from a combination of tip/tilt sensor noise and tilt anisoplanatism. The AO system modeling techniques used to quantify these considerations in terms of the sky coverage function $P(S \geq S_0)$ are described in previous papers.[6,9] together with sample results for the Gemini-North telescope which were computed assuming no uncorrectable telescope aberrations. In this section we investigate how these results are influenced by the representative optical aberrations illustrated in Section 3 above.

The evaluation of AO system sky coverage for a particular observing scenario requires a parameterized family of point spread functions $\mathrm{PSF}(\theta, R)$ which define AO system performance with a natural guide star of magnitude R at an angular offset θ from the science field. Together with a guide star model describing the density of guide stars as a function of their magnitude, this family of PSF's can be used to compute the probability of locating a natural guide star both bright enough and near enough to the science field to achieve a given level of performance. For a LGS AO system, these point spread functions may be computed using the equation

$$\mathrm{PSF}(\theta, R) = \mathrm{PSF}_{\mathrm{ho}} * \mathrm{PSF}_{\mathrm{tt}}(\theta, R). \tag{4.1}$$

Here PSF_{ho} is the short-exposure (tilt removed) PSF due to residual higher order aberrations left uncorrected by the laser guide star AO system, the asterisk denotes the convolution operator, and PSF_{tt} is a Gaussian transfer function which represents the additional blurring in the long-exposure PSF due to residual tip and tilt errors. The short-exposure PSF is independent of the parameters θ and R because the laser guide star used for higher-order correction has constant brightness and can always be projected in the direction of the science object. In terms of this model, unsensed and uncorrectable optical aberrations impact AO system sky coverage by degrading the point spread functions $PSF(\theta, R)$ in two ways:

- The short-exposure PSF and OTF are degraded directly according to Eq. (2.6) above, and
- Blurring of the NGS images in the tracker or Shack-Hartmann sensor used for tip/tilt sensing increases the tilt measurement error due to noise for a fixed NGS magnitude R, consequently increasing the residual tilt jitter and broadening the function PSF_{tt}.

For Gemini, each science instrument is equipped with its own "on-instrument," or colocated. Shack-Hartmann sensor for tip/tilt sensing. The magnitude of the increased tip/tilt jitter due to blurring can be quantified by evaluating the OTF for each sensor subaperture using Eq. (2.6). and then applying standard formulas for quadrant detector tilt measurement accuracy as a function of signal level and the shape of the PSF.[17,18] The same aberration profile can be used for the tip/tilt sensor and the science instrument since the two devices are colocated. In the calculations to date the increased tilt jitter due to blurring of the NGS image has been fairly negligible, and nearly all of the reduction in sky coverage associated with static telescope aberrations has been due to their direct effect upon the higher order point spread function PSF_{ho}.

Fig.'s 10 and 11 illustrate sample results for the effect of uncorrectable aberrations on Gemini-North sky coverage. These results are for an imaging wavelength of 1.65 μm, the LGS AO and observing parameters listed in column 4 of Table 2, a guide star density profile corresponding to the galactic pole, and tip/tilt sensor radiometry parameters as described previously.[6] Fig. 10 quantifies sky coverage in terms of Strehl ratio, while Fig. 11 considers the case of power coupling through a 0.1 arcsec spectrometer slit. In both cases the effect of the uncorrectable aberrations is nonnegligible, but the relative reduction in system performance is smaller for the second case. For example, the typical aberration profile reduces the Strehl ratio for 50 per cent sky coverage from about 0.45 to 0.34, a relative reduction of about 24 per cent. The corresponding values for slit power coupling are about 0.68, 0.59, and 13 per cent. Evidently, the sample noncommon path aberrations used in these calculations contain a range of spatial frequencies which scatter some, but not all, of the central lobe of the PSF outside of the aperture for a 0.1 arcsec slit.

Many different sets of observing conditions and noncommon path aberrations may need to be considered for the design and optimization of an AO system, and it may become computionally cumbersome to repetitively evaluate Eq. (2.6) for each pair. Computation requirement can be reduced by applying Eq. (2.8) or (2.10) to approximate the effect of noncommon path aberrations on the end-to-end Strehl ratio or OTF. Fig.'s 12 and 13 illustrate the effect of these approximations on the final sky coverage predictions for the AO system. Using the multiplicative OTF approximation leads to very modest errors in the sky coverage estimates which are probably small relative to other uncertainties in the calculation.

The errors in sky coverage associated with the multiplicative Strehl ratio approximation are significantly larger, particularly in Fig. 13 where the approximation is applied to slit power coupling instead of the Strehl ratio.

5. Summary

In this paper we have investigated the interaction of static telescope aberrations and residual turbulence-induced phase distortions upon the performance of adaptive optical systems. Multiplicative approximations for the combined effect of these two wave-front error sources upon the time averaged Strehl ratio and OTF of the AO system are remarkably accurate as long as the overall time average Strehl ratio is greater than about 0.1. This result allows the effects of static telescope aberrations to be easily included in AO system sky coverage calculations. A similar approximation for the speckle transfer function can be seriously in error unless the Strehl ratio is greater than about 0.3, at which point speckle imaging methods are generally no longer required.

ACKNOWLEDGMENTS

While the work described in this paper was performed, D. W. Tyler was employed by the Schafer Corporation, Albuquerque, NM, an opportunity for which he is deeply grateful. Myung Cho, Mark Chun, and Jim Oschmann of the Gemini 8-Meter Telescopes Project supplied data on the representative unsensed and uncorrectable mirror figure errors studied in section 3. Comments by the reviewers significantly improved the presentation of the numerical results in section 3. This work was funded by the Air Force Office of Scientific Research. The authors gratefully acknowledge their support.

REFERENCES

1. *Advanced Technology Optical Telescopes V*, Larry M. Stepp, ed., SPIE Proceedings series vol. 2199, Bellingham (1994).
2. *Adaptive Optics in Astronomy*, M. Ealey and F. Merkle, ed., SPIE Proceedings series vol. 2201, Bellingham (1994).
3. J. P. Veran, F. Rigaut, H. Maitre, and D. Rouan, "Estimation of the adaptive optics long-exposure point-spread function using control loop data," J. Opt. Soc. Am. A **14**, pp. 3057–3069 (1997).
4. M.C. Roggemann and C.L. Matson, "Power spectrum and Fourier phase spectrum estimation by using fully and partially compensating adaptive optics and bispectrum postprocessing," J. Opt. Soc. Am. A **9**, pp. 1525–1535 (1992).
5. F. Rigaut, B. L. Ellerbroek, and M. J. Northcott, "Comparison of Adaptive-Optics Technologies for Large Astronomical Telescopes," Appl. Opt. **36**, 2856–2864 (1997).
6. B. L. Ellerbroek and D. W. Tyler, "Adaptive Optics Sky Coverage Calculations for the Gemini-North Telescope," Proc. Ast. Soc. Pac. **110**, pp. 165–185 (1998).
7. F. Rigaut and E. Gendron, "Dual adaptive optics, a solution to the tilt determination problem using laser guide star," in *Laser Guide Star Adaptive Optics Workshop*, R. Fugate. ed., pp. 582–590, Starfire Optical Range, Albuquerque (1992).
8. N. Hubin, B. Theodore, P. Petitjean and B. Delabre, "Adaptive optics system for the Very Large Telescope," in *Adaptive Optics in Astronomy*, M. Ealey and F. Merkle, ed., SPIE Proceedings series vol. 2201, pp. 34–45, Bellingham (1994).
9. D. W. Tyler and B. L. Ellerbroek, "Spectrometer slit-power-coupling calculations for natural and laser guide-star adaptive optics," Appl. Opt. **37**, pp. 4569–4576 (1998).
10. J. W. Goodman, "Frequency analysis of optical imaging systems," in *Introduction to Fourier Optics*, pp. 101–133, McGraw-Hill, San Francisco (1968).
11. R. E. Hufnagel and N. R. Stanley, "Modulation transfer function associated with transmission through turbulent media," JOSA **54**, pp. 52–61 (1964).
12. M. Born and E. Wolf, "The diffraction theory of aberrations," in *Principles of Optics*, 6 ed., pp. 459–490, Pergamon Press, Sydney (1989).
13. V. N. Mahajan, "Random aberrations," in *Aberration Theory Made Simple*, pp. 135–149, SPIE Tutorial Text Series 06, Bellingham, WA (1991).
14. T. Nakajima. C.A. Haniff, "Partial adaptive compensation and passive interferometry with large ground-based telescopes," Proc. Ast. Soc. Pac. **105**, pp. 509–520 (1993).
15. B. L. Ellerbroek, "First-order performance evaluation of adaptive optics systems for atmospheric turbulence compensation in extended field-of-view astronomical telescopes," J. Opt. Soc. Am. A **11**, 783–805, 1994.
16. D. W. Tyler and B. L. Ellerbroek, "Sky coverage calculations for spectrometer slit power coupling with adaptive optics compensation," in *Adaptive Optical System Technologies*, D. Bonaccini and R. K. Tyson, ed., SPIE Proceedings series vol. 3353, pp. 201-209, Bellingham (1998).
17. G. A. Tyler and D. L. Fried, "Image position error associated with a quadrant detector," J. Opt. Soc. Am. **72**, pp. 804–808 (1992).
18. B. M. Welsh, B. L. Ellerbroek, M. C. Roggemann, and T. L. Pennington, "Shot noise performance of Hartmann and shearing interferometer wave front sensors," in *Adaptive*

Optical Systems and Applications, R. K. Tyson and R. Q. Fugate, ed., SPIE Proceedings series vol. 2534, pp. 277–288, Bellingham (1995).

TABLES

Scenario	1	2	3	4
Aperture diameter, m	1.0	1.0	1.0	7.9
Linear obscuration ratio	0.0	0.0	0.0	0.152
Imaging wavelength, μm	1.06	1.06	1.06	1.65
AO guide star	NGS	NGS	NGS	LGS at $z = 92.5$ km
WFS Subapertures	8×8	8×8	8×8	12×12
DM Actuators	9×9	9×9	9×9	13×13
AO loop bandwidth, Hz	∞	∞	∞	100
Turbulence Profile	$HV_{5/7}$	$HV_{5/7}$	$HV_{5/7}$	Typical Mauna Kea, $\psi = 0°$
Static Aberrations	Focus	Focus	Focus	Simulated Gemini-North aberrations
Fitting error, d/r_0	1–4	1	1	0.67
WFS noise, $\sigma_\theta/(\lambda/d)$	0.0	0.0–0.4	0.0	0.0
Anisoplanatism, θ/θ_0	0	0	0–2	0

Table 1. Parameter values for OTF and Strehl ratio calculations. Here NGS denotes a natural guide star. LGS an artifically generated laser guide star at range z, ψ is the zenith angle, d is the width of a WFS subaperture, r_0 is the turbulence-induced atmospheric coherence diameter, σ_θ is the RMS WFS subaperture tilt measurement accuracy, λ is the imaging wavelength, θ is the angular offset between the guide star and the science object, and θ_0 is the isoplanatic angle. The notation "$HV_{5/7}$" denotes the Hufnagel-Valley turbulence profile scaled to yield $r_0 = 5$ cm and $\theta_0 = 7\,\mu$rad at $\lambda = 0.5\,\mu$m. Futher description of these parameters is contained in the text.

Phase Errors	Computation	Strehl ratio		
		1.25 μm	1.65 μm	2.20 μm
Turbulence	Exact	0.621	0.760	0.856
Typical aberrations	Exact	0.568	0.708	0.818
Best case aberrations	Exact	0.762	0.852	0.913
Turbulence and typical aberrations	Exact	0.365	0.545	0.703
	Multiplicative	0.353	0.538	0.700
Turbulence and best case aberrations	Exact	0.481	0.651	0.783
	Multiplicative	0.473	0.648	0.782

Table 2. Strehl ratio results for Gemini-North telescope and AO system parameters. This table lists Strehl ratios computed in three astronomical imaging bands based on the Gemini system parameters listed in the last column of Table 1. The first section of the table lists Strehl ratios computed separately for the effects of atmospheric turbulence and optical system aberrations. The remaining two sections of the table lists Strehl ratios for the combined effect of these two error sources, where the "exact" values have been computed using Eq. (2.7), and the "multiplicative" values are derived from the first section of the table using Eq. (2.9). The multiplicative approximation is accurate to within a few per cent over the range of cases considered.

FIGURES

Fig. 1. Representative unsensed and uncorrectable mirror figure errors for the Gemini-North Telescope. This phase error profile yields a Strehl ratios of about 0.66 at a wavelength of 1.65 μm , which corresponds roughly to the Gemini specification for mirror figure errors and misalignments. The profile is a sum of contributions due to primary and secondary mirror polishing and mounting errors, together with noncommon path aberrations between the WFS and the science instrument. The mirror figure errors have been studied in considerable detail by Gemini, but the noncommon path errors used here are merely "typical" values selected to match the overall Strehl ratio given above. A more benign profile corresponding to an overall Strehl ratio of about 0.82 has also been considered.

Fig. 2. Strehl ratio calculations for representative AO system parameters and wave-front errors. These curves plot the exact Strehl ratio and its multiplicative approximation computed for the AO system parameters and static and varying wave-front errors summarized in columns 1 through 3 of Table 1. Subfigure (a) plots results for wave-front errors dominated by DM fitting error with $d/r_0 = 1$ (top). 2, and 4 (bottom), subfigure (b) is for the case of WFS noise with $\sigma_\theta/(\lambda/d) = 0$ (top). 0.1. 0.2, and 0.4 (bottom), and subfigure (c) is for anisoplanatic wave-front errors with $\theta/\theta_0 = 0$ (top). 0.5. 1, and 2 (bottom). In subfigure (a), the results for the multiplicative approximation overlay the exact Strehl ratios to within the resolution of the plot. See the caption to Table 1 for the definitions of these variables.

Fig. 3. OTF reduction due to a static focus aberration of 0.7 radians RMS.

Fig. 4. OTF calculations for representative AO system parameters and wave-front errors. These OTF's correspond to the AO system parameters and turbulence-induced wave-front errors described in the caption to Fig. 2 above, combined with a static focus error with a magnitude of 0.7 radians RMS.

Fig. 5. STF calculations for wave-front fitting error with $d/r_0 = 1$, 2, and 4, and the AO system parameters listed in column 1 of Table 1. Exact STF's and multiplicative approximations are shown for a static focus error of 0.2 radians RMS (Fig. 5a), 0.7 radians RMS (Fig. 5b), and 1 radian RMS (Fig. 5c).

Fig. 6. STF calculations for anisoplanatic wave-front errors with $\theta/\theta_0 = 0.5$, 1, and 2, and the AO system parameters listed in column 2 of Table 1.

Fig. 7. STF's for diffraction-limited imaging, residual atmospheric wave-front error only, and static focus wave-front error only cases. The atmospheric wave-front error is due to anisoplanatism with $\theta/\theta_0 = 1$ (Fig. 7a) and $\theta/\theta_0 = 2$ (Fig 7b). AO system parameters are as listed in column 3 of Table 1. The static error is due to a 0.7-radian RMS focus error. Exact and approximate STF's are also shown for the combination of the two effects.

Fig. 8. OTF calculations for Gemini-North AO system parameters and wave-front errors. These OTF's correspond to the Gemini AO system parameters and turbulence-induced phase errors summarized in the final column of Table 1, combined with typical and best-case unsensed and uncorrectable optical system aberrations. The wavelength is 1.65 μm. The OTF's are very well approximated by the product of terms computed separately for the two error sources.

Fig. 9. STF's for diffraction-limited imaging, residual atmospheric wave-front error only, and static telescope wave-front error only cases. The atmospheric wave-front error is due to nominal residual phase at 1.2 μm for the Gemini AO system parameters. The static error is due to the "typical case" Gemini optical aberrations. Exact and approximate STF's are also shown for the combination of the two effects. Because the Gemini aberrations are not symmetric, all plots are radial averages of two-dimensional distributions.

Fig. 10. Impact of uncorrectable telescope aberrations on Strehl ratio sky coverage for Gemini-North at an observing wavelength of 1.65 μm. Here "sky coverage" is defined as the fraction of the sky close enough to a sufficiently bright guide star for the AO system to deliver the indicated Strehl ratio. The uncorrectable telescope aberrations used for these calculations are as illustrated in Fig. 1, and the AO system and observing parameters are listed in column 4 of Table 2. Information on the guide star density model and tip/tilt sensor radiometry parameters can be found in a previous paper.[5]

Fig. 11. Impact of uncorrectable telescope aberrations on slit power coupling sky coverage for Gemini-North. This figure is similar to Fig. 10, except that AO system performance is described in terms of the fraction of energy from a point source which is transmitted through a 0.1 arcsec spectrometer slit.

Fig. 12. Effect of approximations on estimated Strehl ratio sky coverage for Gemini-North. This figure illustrates how sky coverage predictions for Gemini-North are effected if the end-to-end performance of the AO system is estimated using one of the two approximations given at the end of Section 2 above. The observing, AO system, and guide star parameters used for these calculations are the same as for Fig. 9 above, along with the larger of the two values for uncorrectable telescope aberrations.

Fig. 13. Effect of approximations on estimated slit power coupling sky coverage for Gemini-North. This figure is similar to Fig. 12, except that AO system performance is described in terms of the fraction of energy from a point source which is transmitted through a 0.1 arcsec spectrometer slit. The results labelled "multiplicative Strehl ratio approximation" were obtained by multiplying the slit power coupling without telescope aberrations by the Strehl ratio due to these aberrations alone.

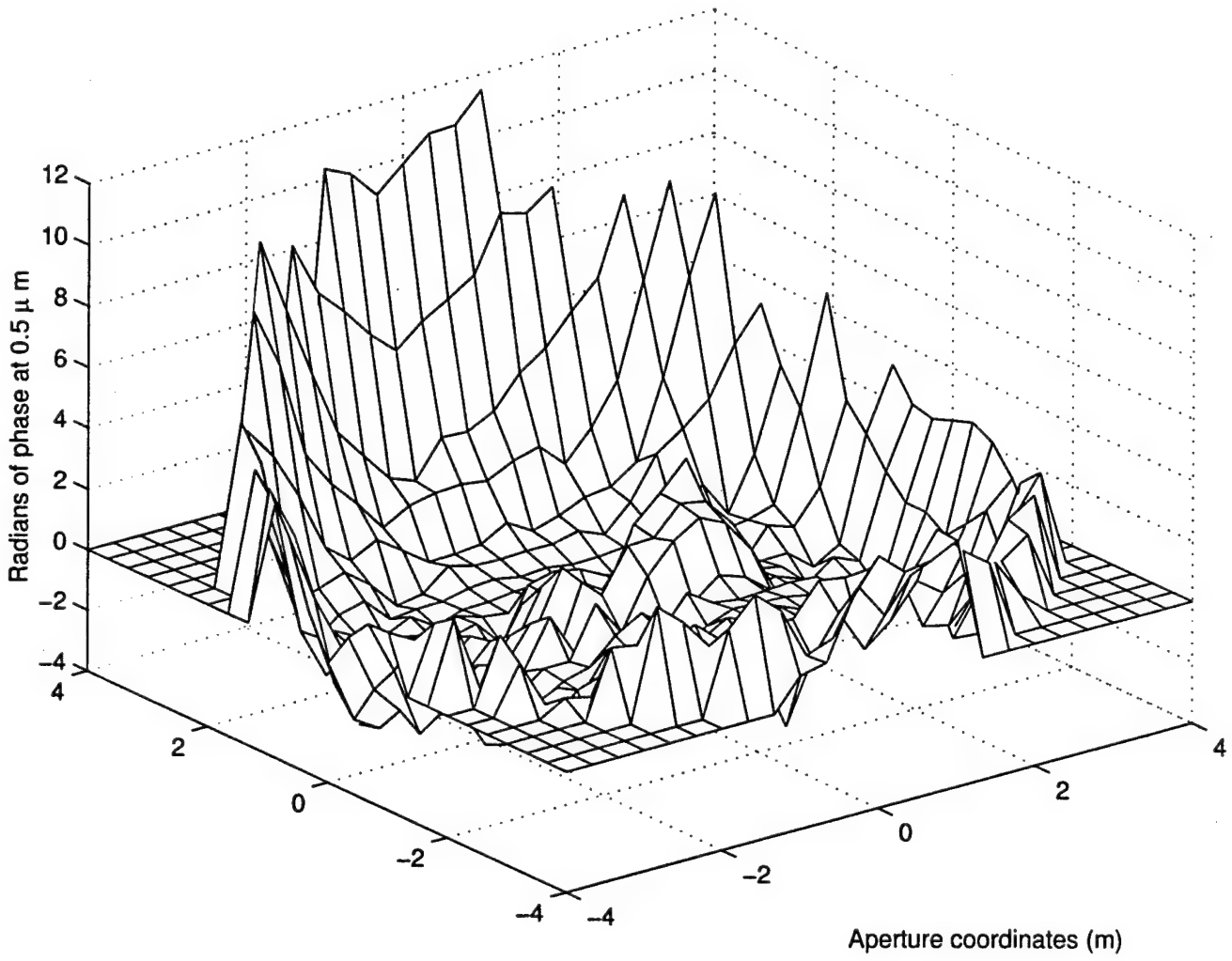
Radians of phase at 0.5 μ m
12
10
8
6
4
2
0
−2
−4
4
2
0
−2
−4
−4
−2
0
2
4
Aperture coordinates (m)

Figure 1

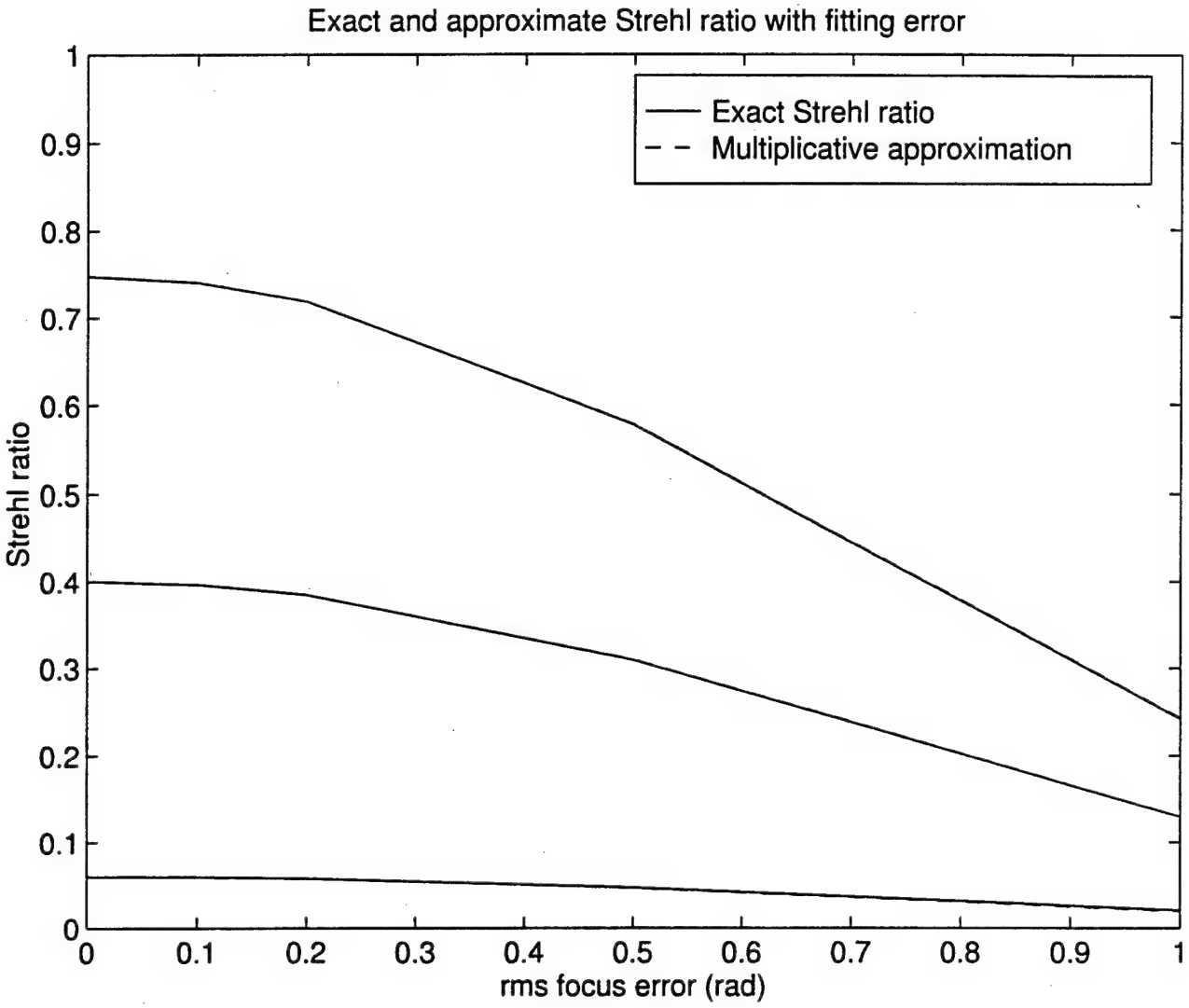
Exact and approximate Strehl ratio with fitting error
Exact Strehl ratio
Multiplicative approximation
Strehl ratio
rms focus error (rad)
0
0.1
0.2
0.3
0.4
0.5
0.6
0.7
0.8
0.9
1

Figure 2a

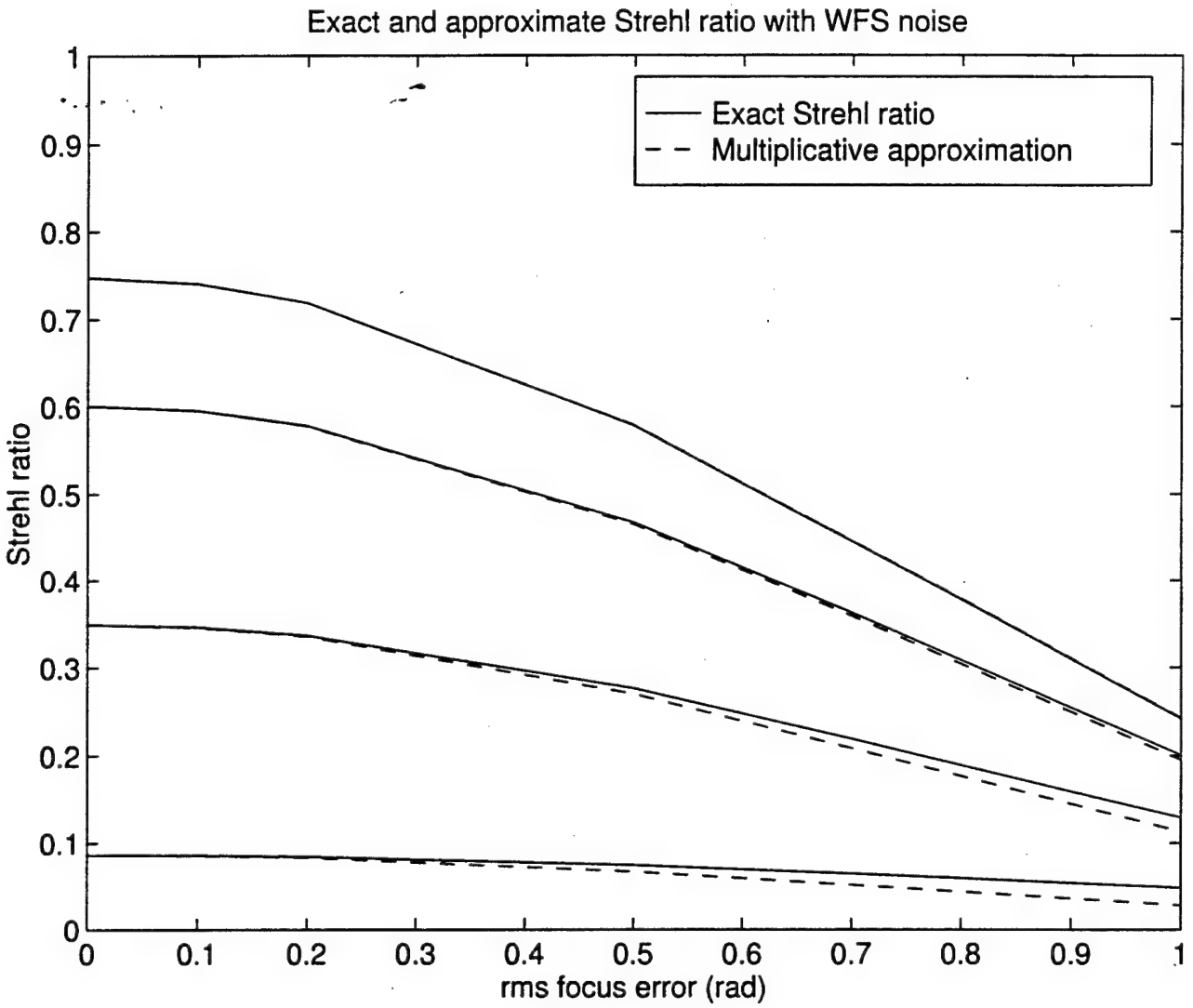
Exact and approximate Strehl ratio with WFS noise
Exact Strehl ratio
Multiplicative approximation
Strehl ratio
rms focus error (rad)
0
0.1
0.2
0.3
0.4
0.5
0.6
0.7
0.8
0.9
1

Figure 2b

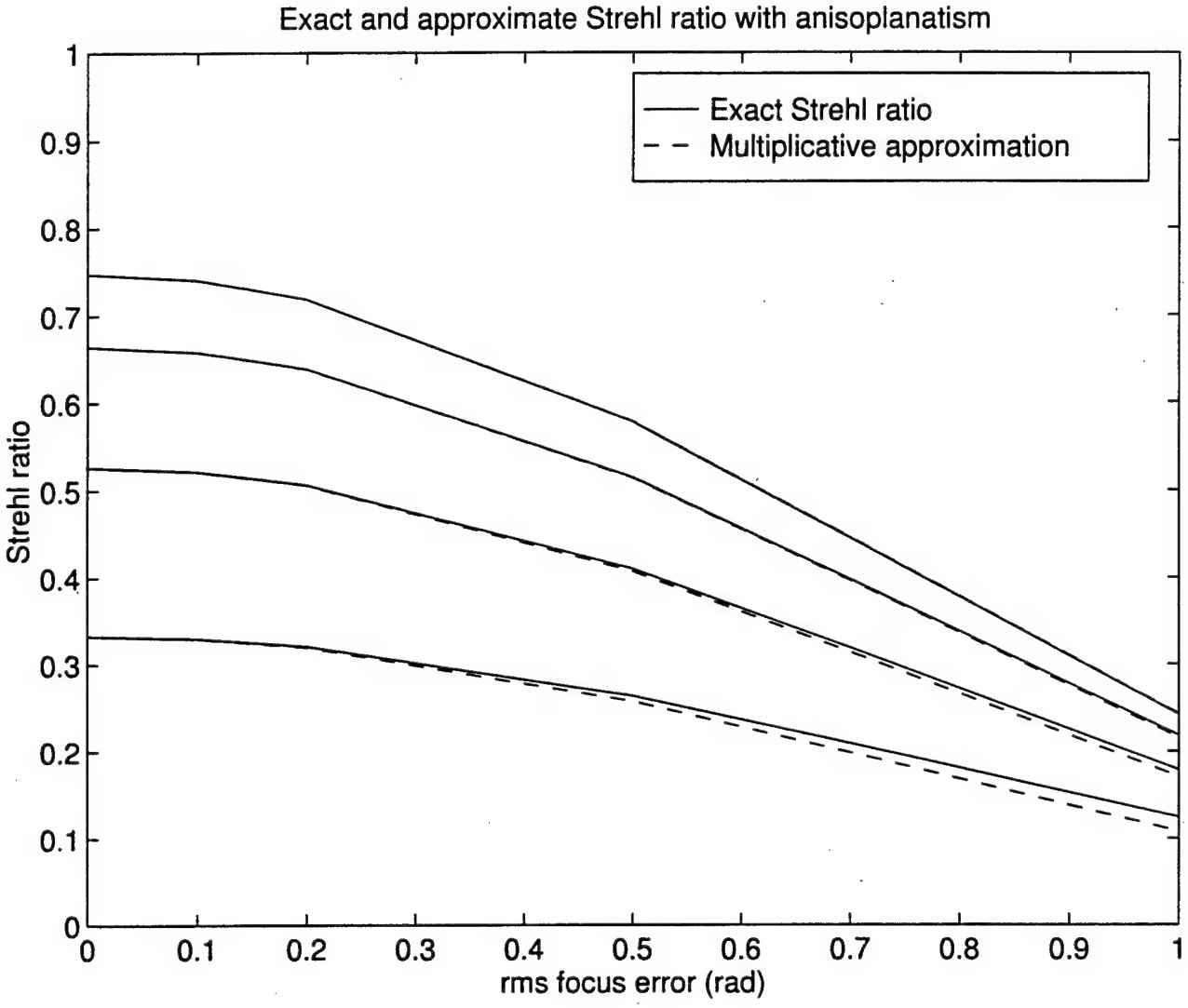
Exact and approximate Strehl ratio with anisoplanatism
Exact Strehl ratio
Multiplicative approximation
Strehl ratio
rms focus error (rad)
0
0.1
0.2
0.3
0.4
0.5
0.6
0.7
0.8
0.9
1

Figure 2c

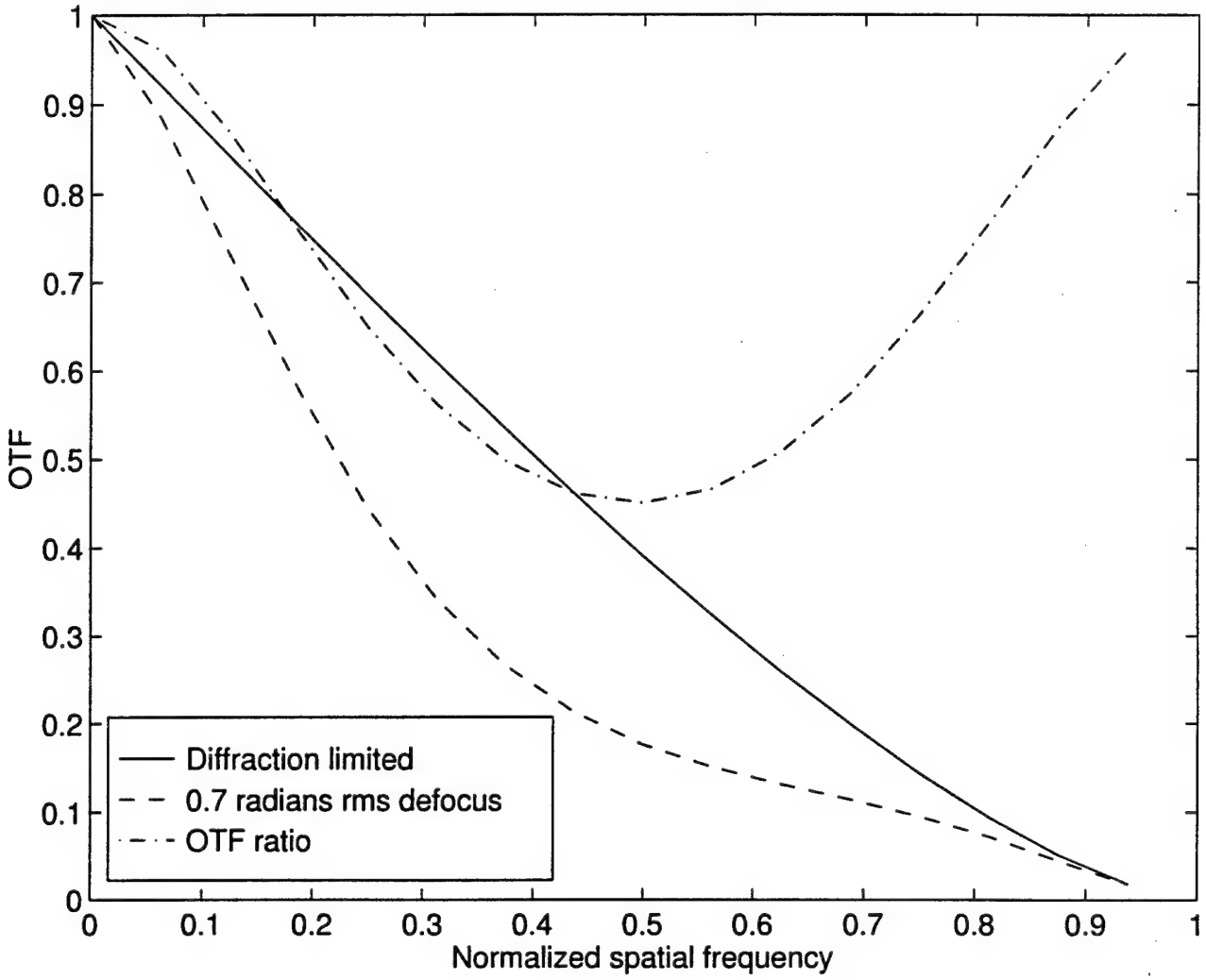
OTF
Normalized spatial frequency
Diffraction limited
0.7 radians rms defocus
OTF ratio
0
0.1
0.2
0.3
0.4
0.5
0.6
0.7
0.8
0.9
1

Figure 3

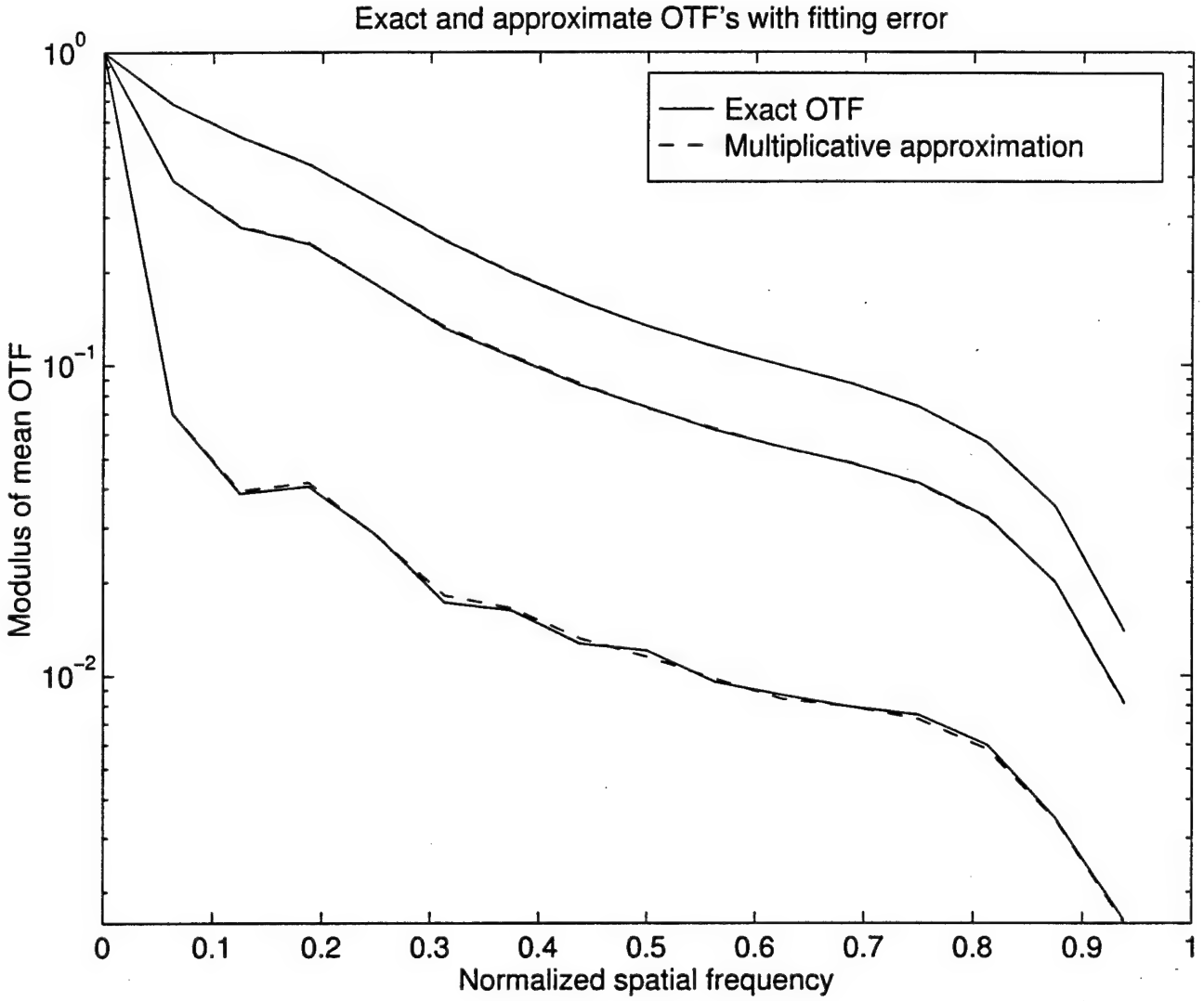
Exact and approximate OTF's with fitting error
Exact OTF
Multiplicative approximation
Modulus of mean OTF
10^0
10^{-1}
10^{-2}
0
0.1
0.2
0.3
0.4
0.5
0.6
0.7
0.8
0.9
1
Normalized spatial frequency

Figure 4a

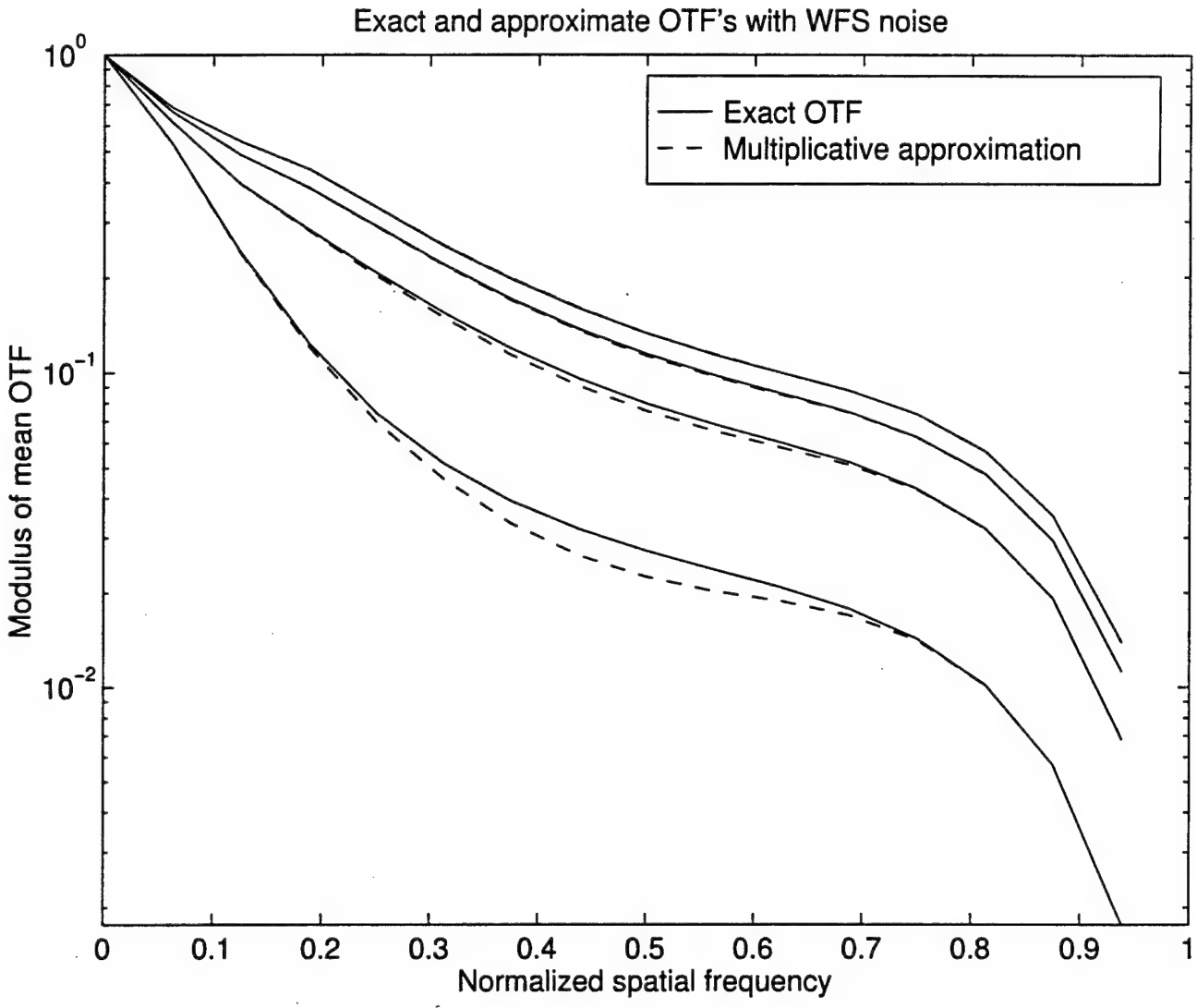
Exact and approximate OTF's with WFS noise
Exact OTF
Multiplicative approximation
Modulus of mean OTF
10^0
10^{-1}
10^{-2}
0
0.1
0.2
0.3
0.4
0.5
0.6
0.7
0.8
0.9
1
Normalized spatial frequency

Figure 4b

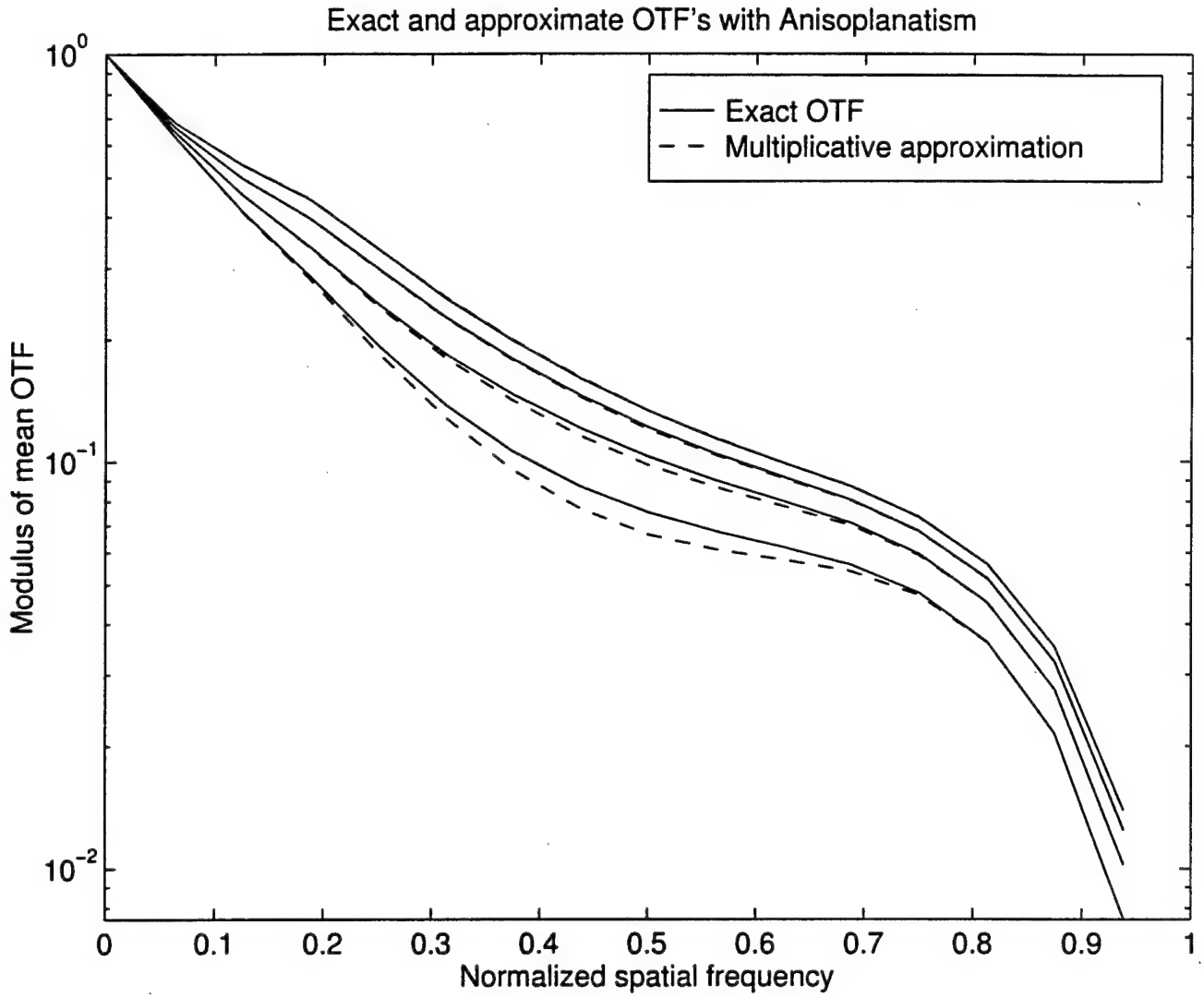
Exact and approximate OTF's with Anisoplanatism
Exact OTF
Multiplicative approximation
Modulus of mean OTF
10^0
10^{-1}
10^{-2}
0
0.1
0.2
0.3
0.4
0.5
0.6
0.7
0.8
0.9
1
Normalized spatial frequency

Figure 4c

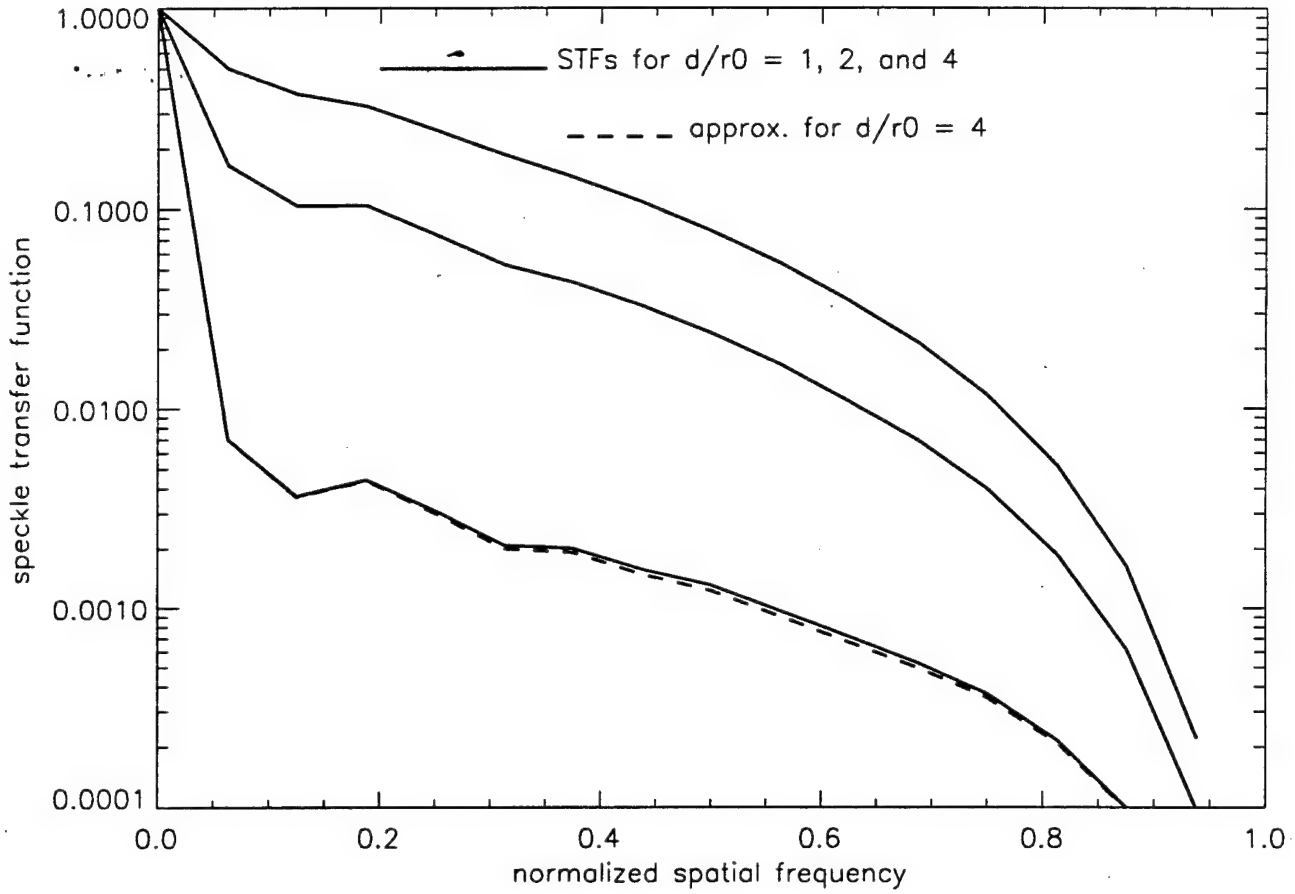
1.0000
0.1000
0.0100
0.0010
0.0001
speckle transfer function
STFs for d/r0 = 1, 2, and 4
approx. for d/r0 = 4
0.0
0.2
0.4
0.6
0.8
1.0
normalized spatial frequency

Fig. 5a

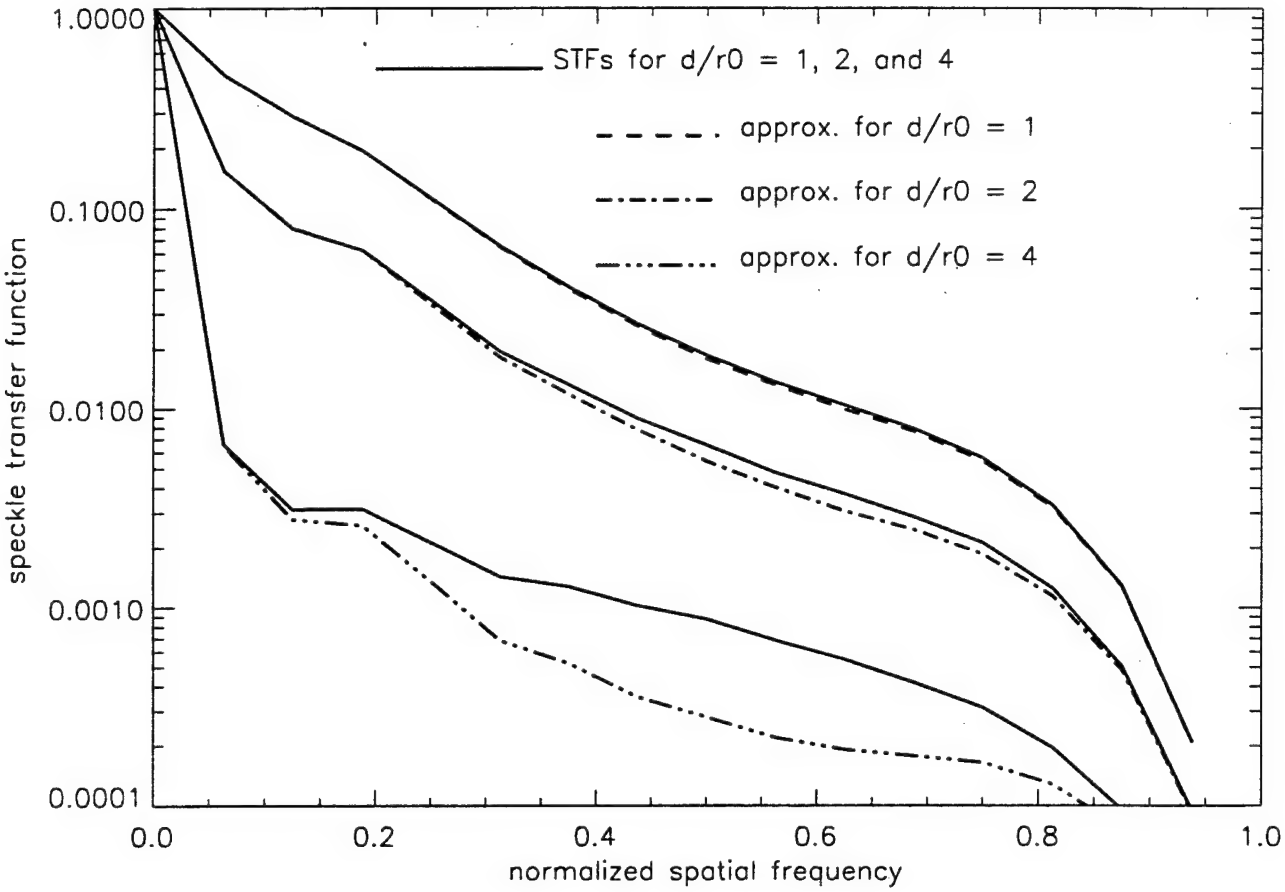
1.0000
0.1000
0.0100
0.0010
0.0001
speckle transfer function
STFs for d/r0 = 1, 2, and 4
approx. for d/r0 = 1
approx. for d/r0 = 2
approx. for d/r0 = 4
0.0
0.2
0.4
0.6
0.8
1.0
normalized spatial frequency

Fig. 5b

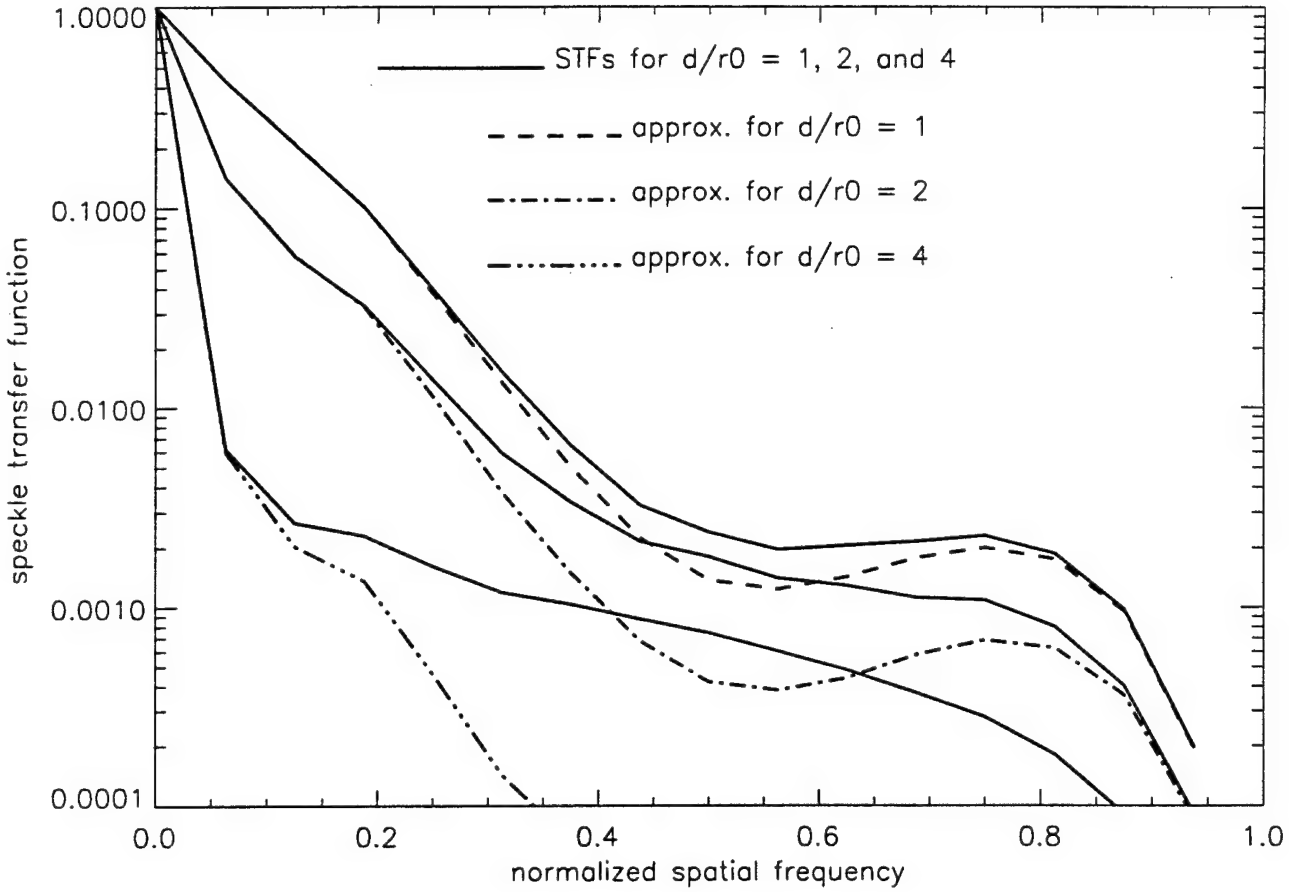
1.0000
0.1000
0.0100
0.0010
0.0001
speckle transfer function
0.0
0.2
0.4
0.6
0.8
1.0
normalized spatial frequency
STFs for d/r0 = 1, 2, and 4
approx. for d/r0 = 1
approx. for d/r0 = 2
approx. for d/r0 = 4

Fig. 5c

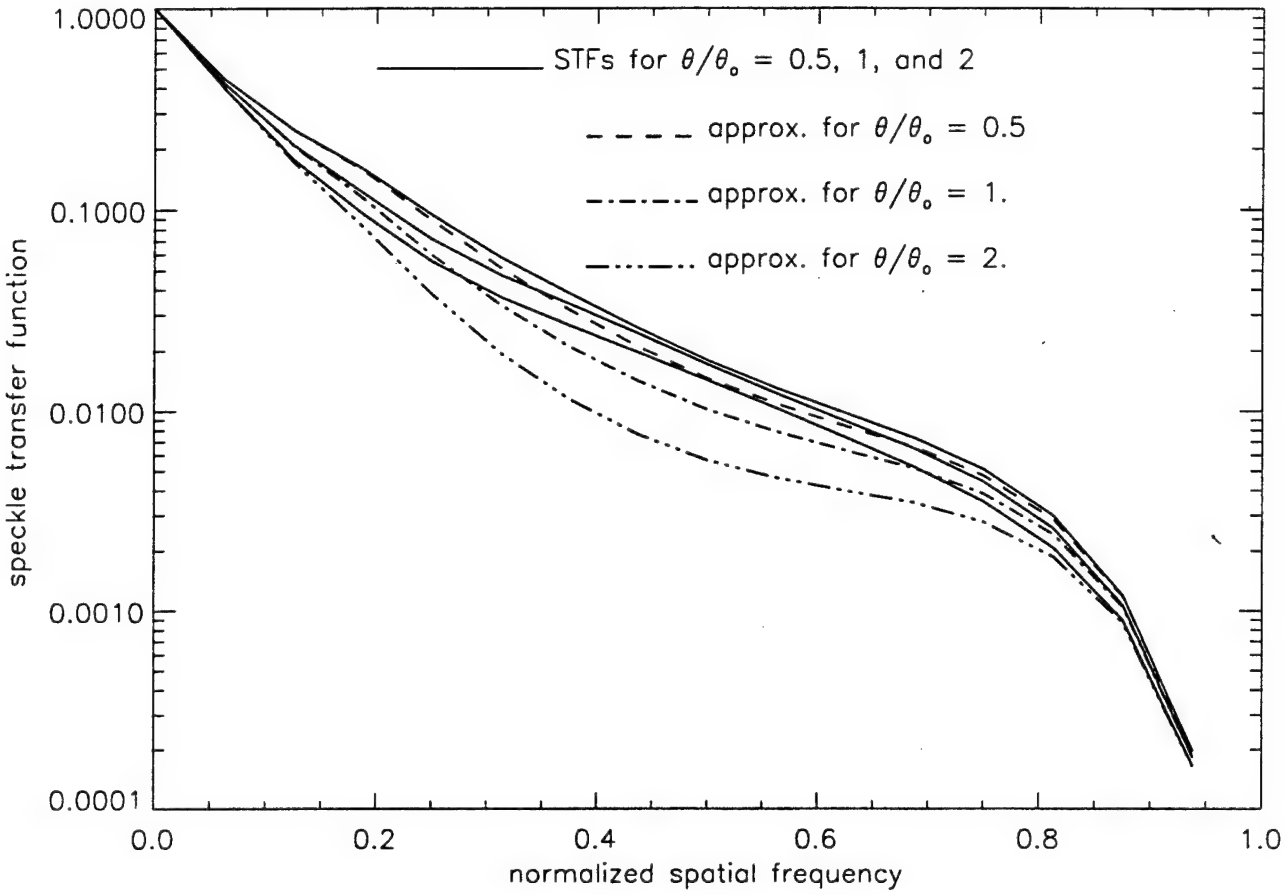
1.0000
0.1000
0.0100
0.0010
0.0001
0.0
0.2
0.4
0.6
0.8
1.0
speckle transfer function
normalized spatial frequency
STFs for θ/θ₀ = 0.5, 1, and 2
approx. for θ/θ₀ = 0.5
approx. for θ/θ₀ = 1.
approx. for θ/θ₀ = 2.

Fig. 6

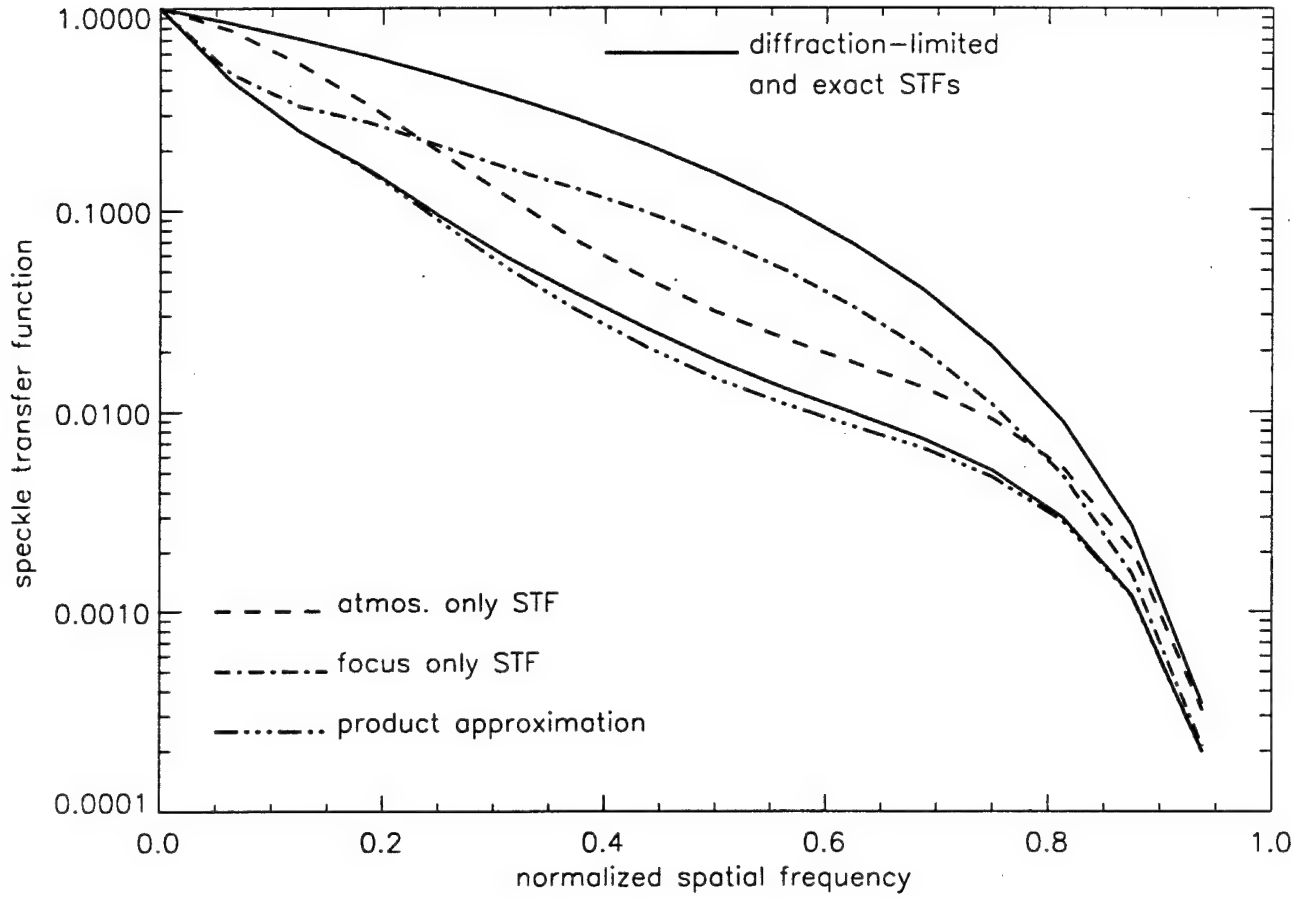
1.0000
0.1000
0.0100
0.0010
0.0001
speckle transfer function
diffraction–limited
and exact STFs
atmos. only STF
focus only STF
product approximation
0.0
0.2
0.4
0.6
0.8
1.0
normalized spatial frequency

Fig. 7a

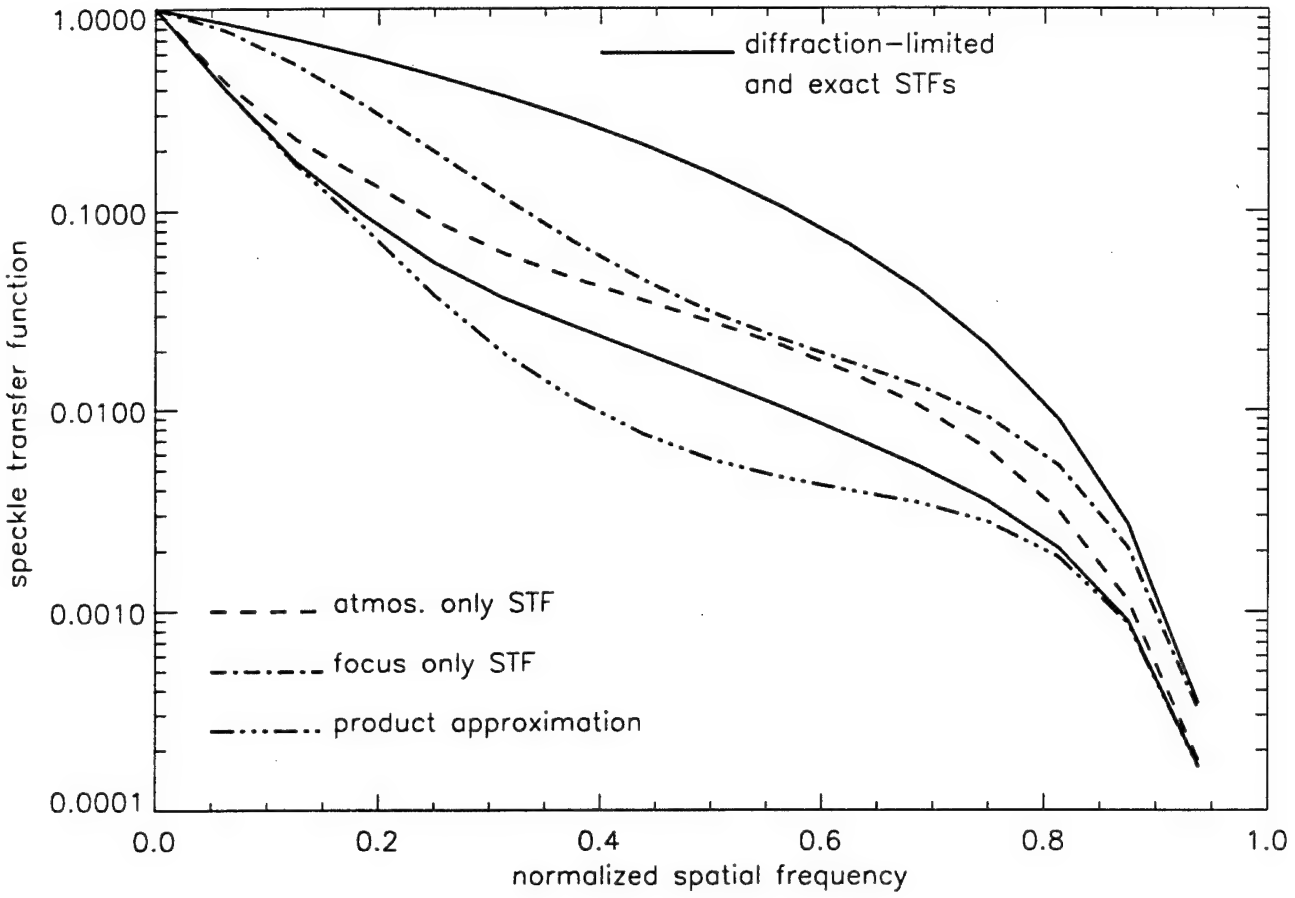
1.0000
0.1000
0.0100
0.0010
0.0001
speckle transfer function
0.0
0.2
0.4
0.6
0.8
1.0
normalized spatial frequency
diffraction–limited
and exact STFs
atmos. only STF
focus only STF
product approximation

Fig. 7b

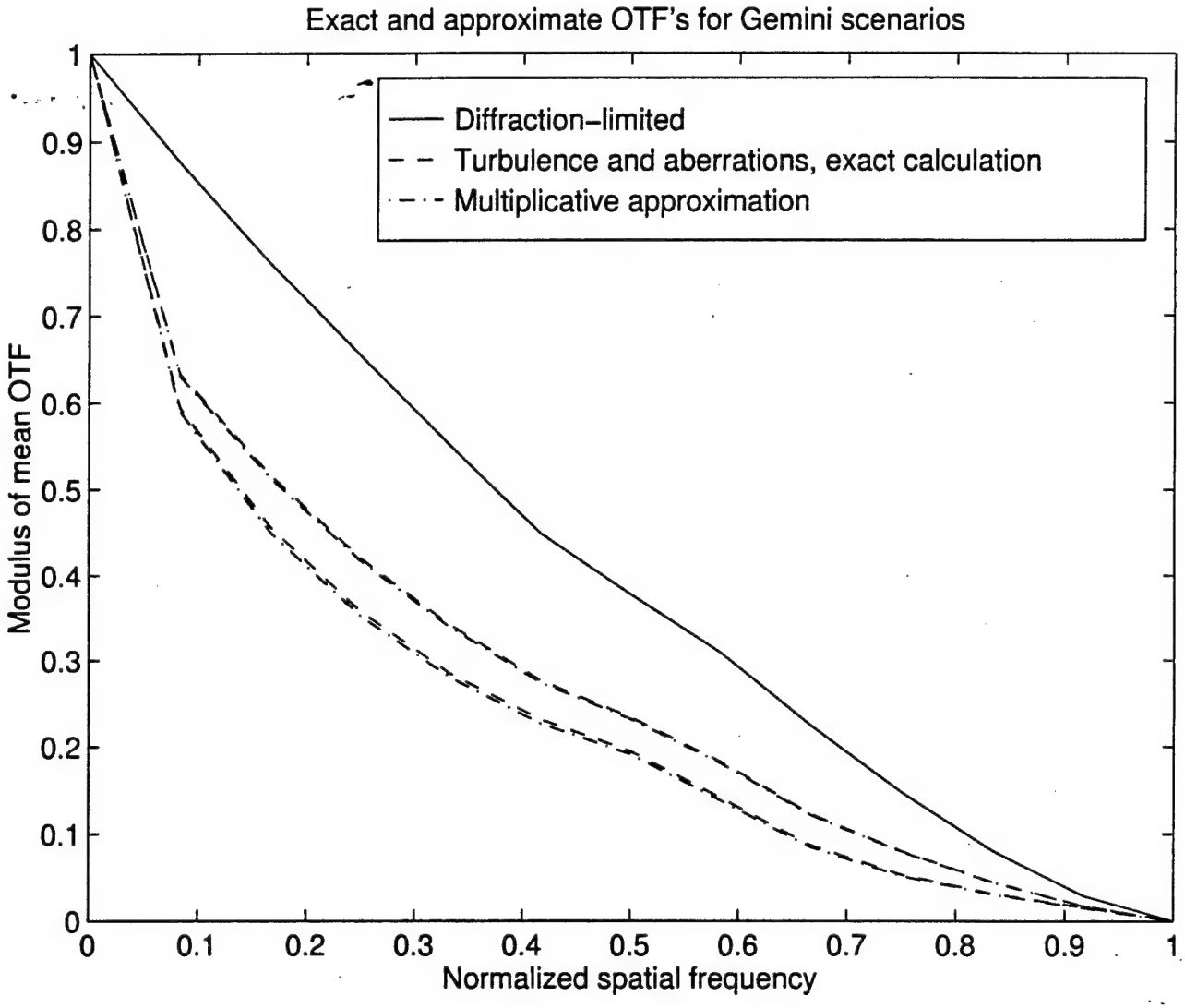
Exact and approximate OTF's for Gemini scenarios
Diffraction–limited
Turbulence and aberrations, exact calculation
Multiplicative approximation
Modulus of mean OTF
Normalized spatial frequency
0
0.1
0.2
0.3
0.4
0.5
0.6
0.7
0.8
0.9
1

Figure 8

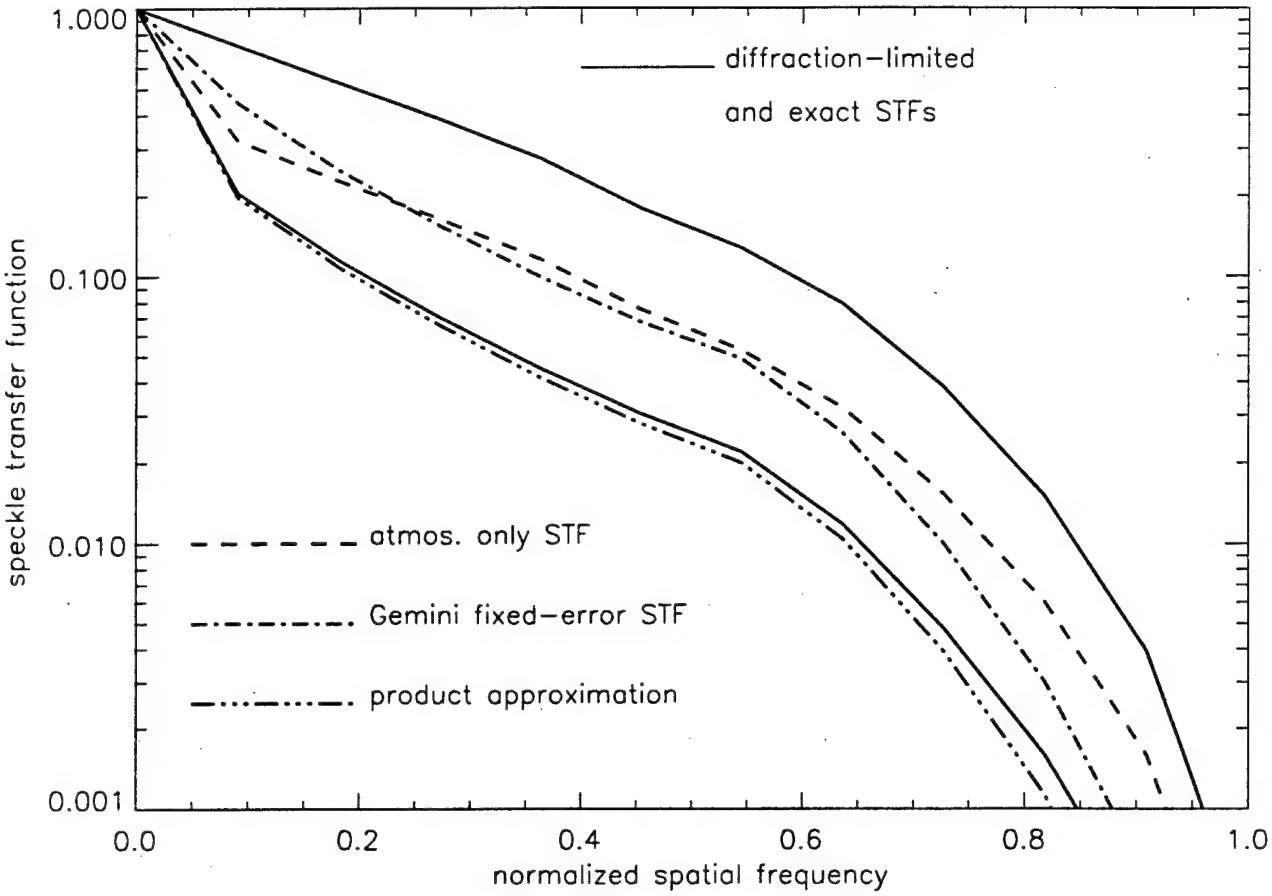
1.000
0.100
0.010
0.001
speckle transfer function
0.0
0.2
0.4
0.6
0.8
1.0
normalized spatial frequency
diffraction–limited
and exact STFs
atmos. only STF
Gemini fixed–error STF
product approximation

Fig. 9

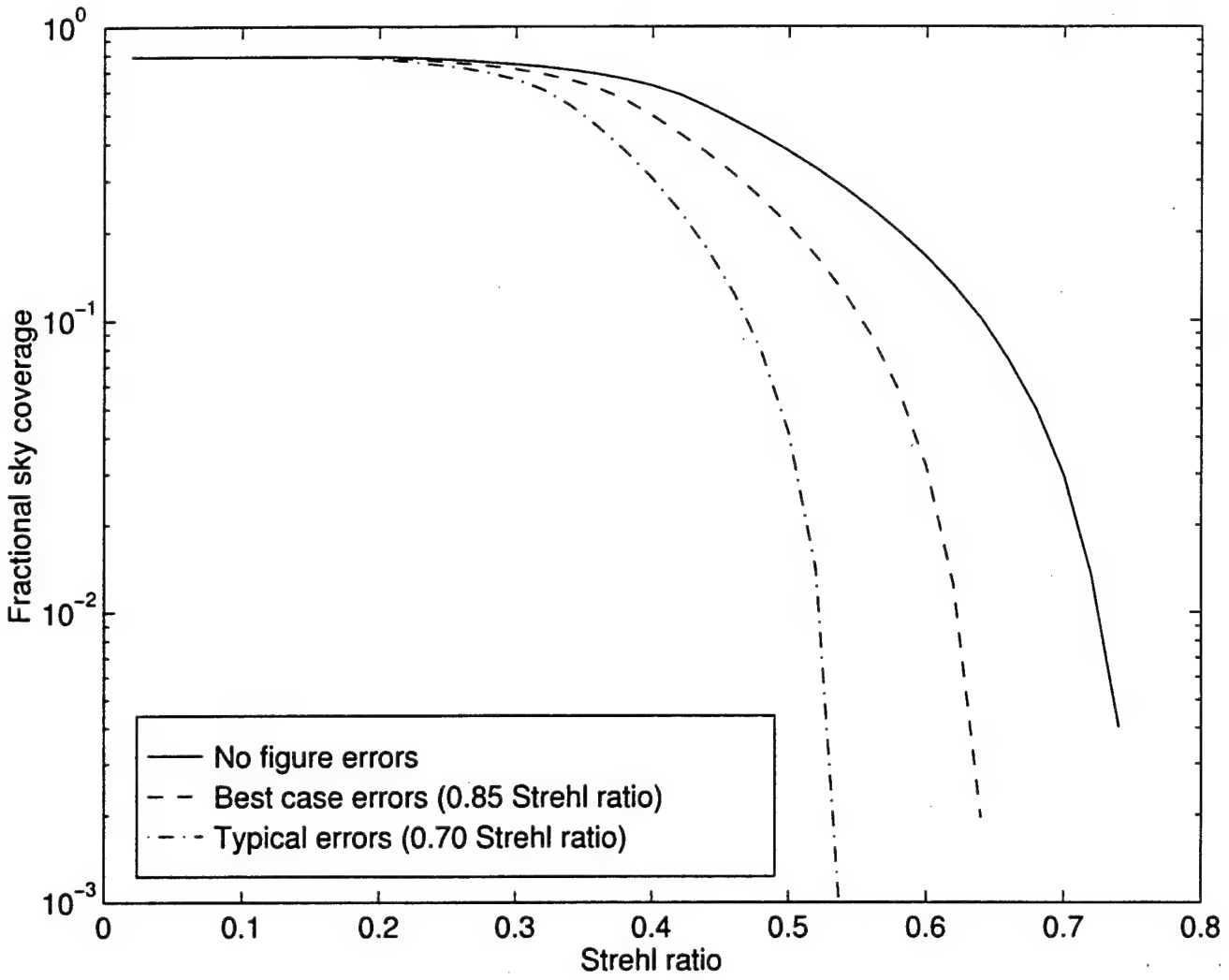
10^0
10^{-1}
10^{-2}
10^{-3}
Fractional sky coverage
0
0.1
0.2
0.3
0.4
0.5
0.6
0.7
0.8
Strehl ratio
No figure errors
Best case errors (0.85 Strehl ratio)
Typical errors (0.70 Strehl ratio)

Figure 10

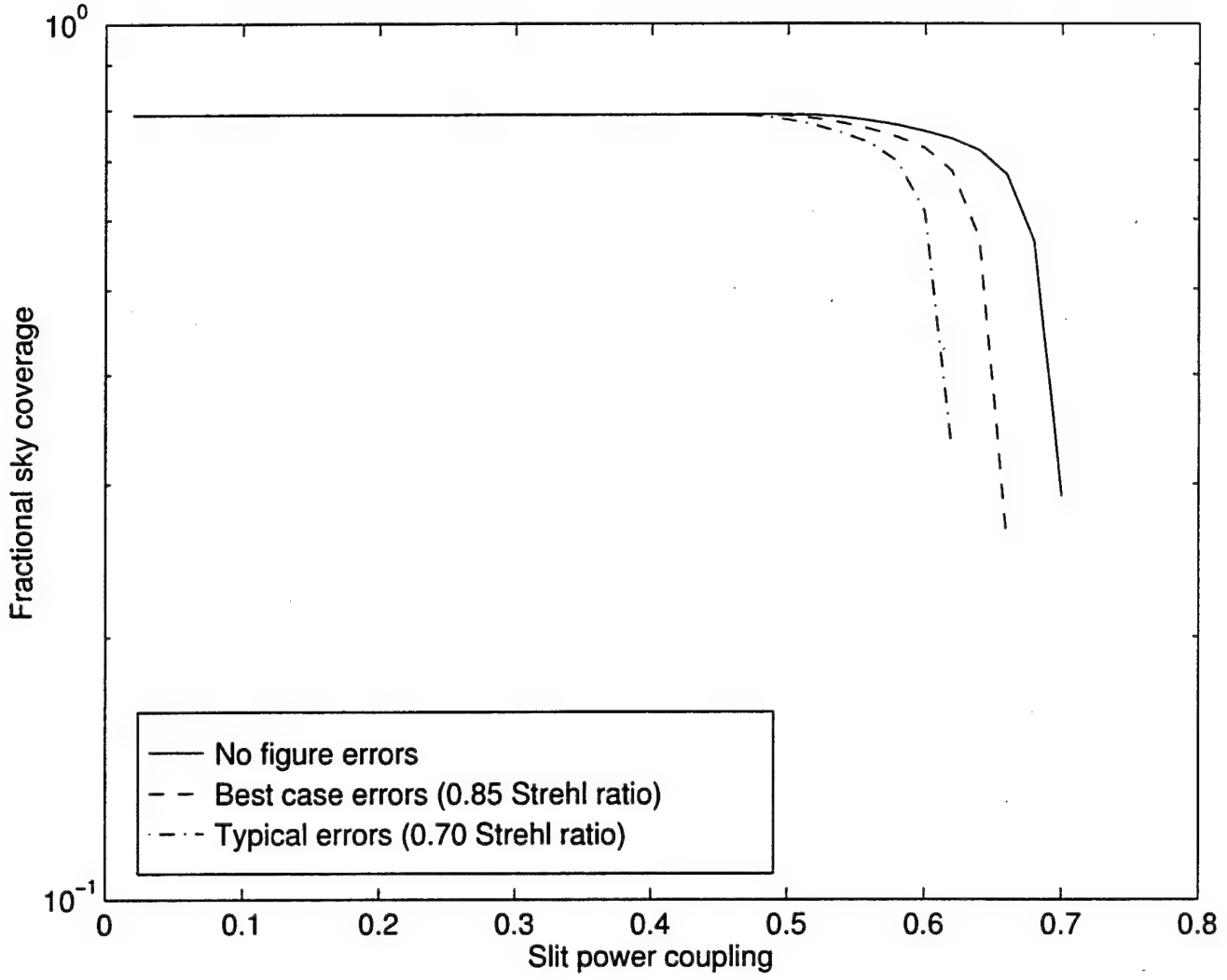
10^0
10^{-1}
Fractional sky coverage
0
0.1
0.2
0.3
0.4
0.5
0.6
0.7
0.8
Slit power coupling
No figure errors
Best case errors (0.85 Strehl ratio)
Typical errors (0.70 Strehl ratio)

Figure 11

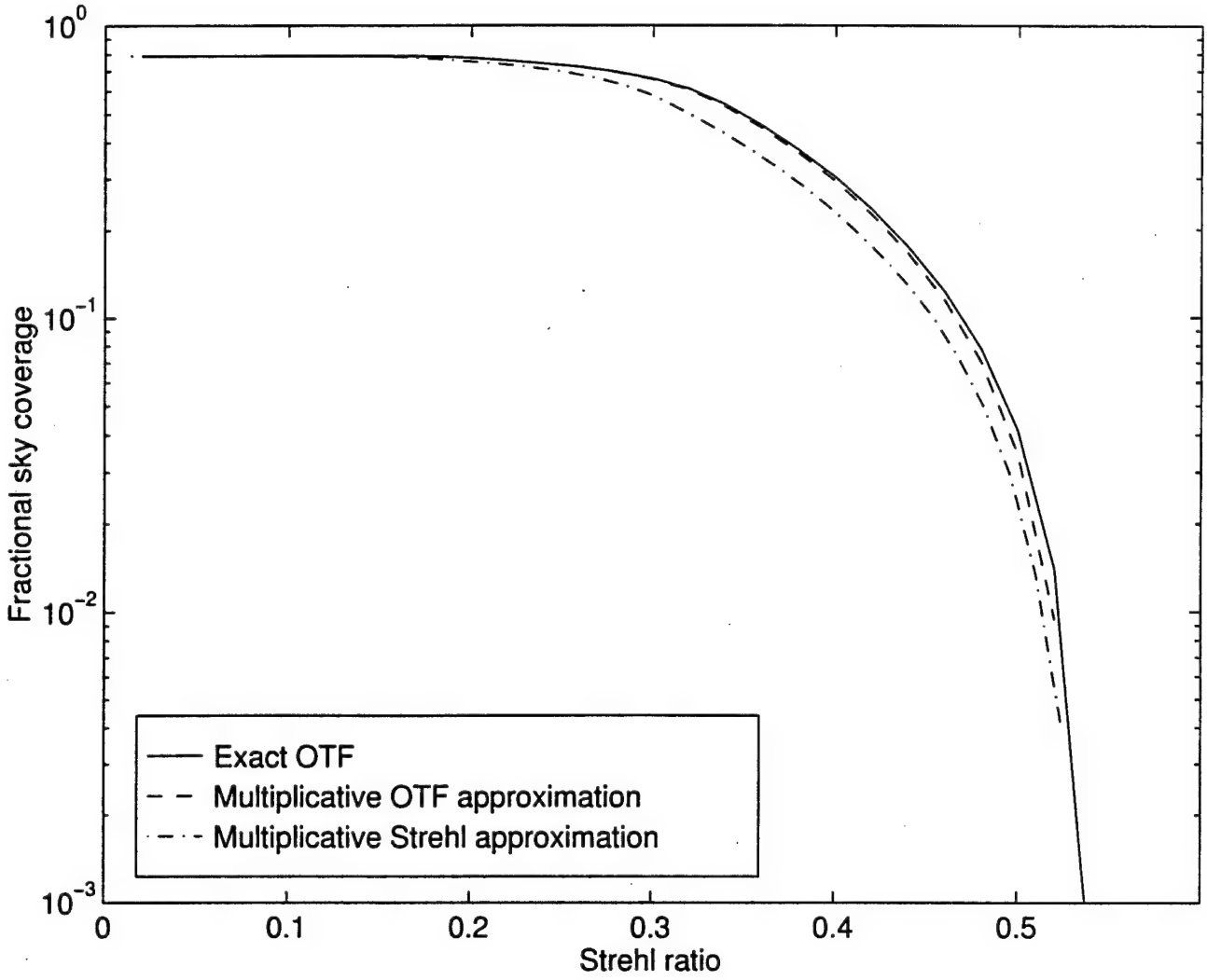
10^0
10^{-1}
10^{-2}
10^{-3}
Fractional sky coverage
0
0.1
0.2
0.3
0.4
0.5
Strehl ratio
Exact OTF
Multiplicative OTF approximation
Multiplicative Strehl approximation

Figure 12

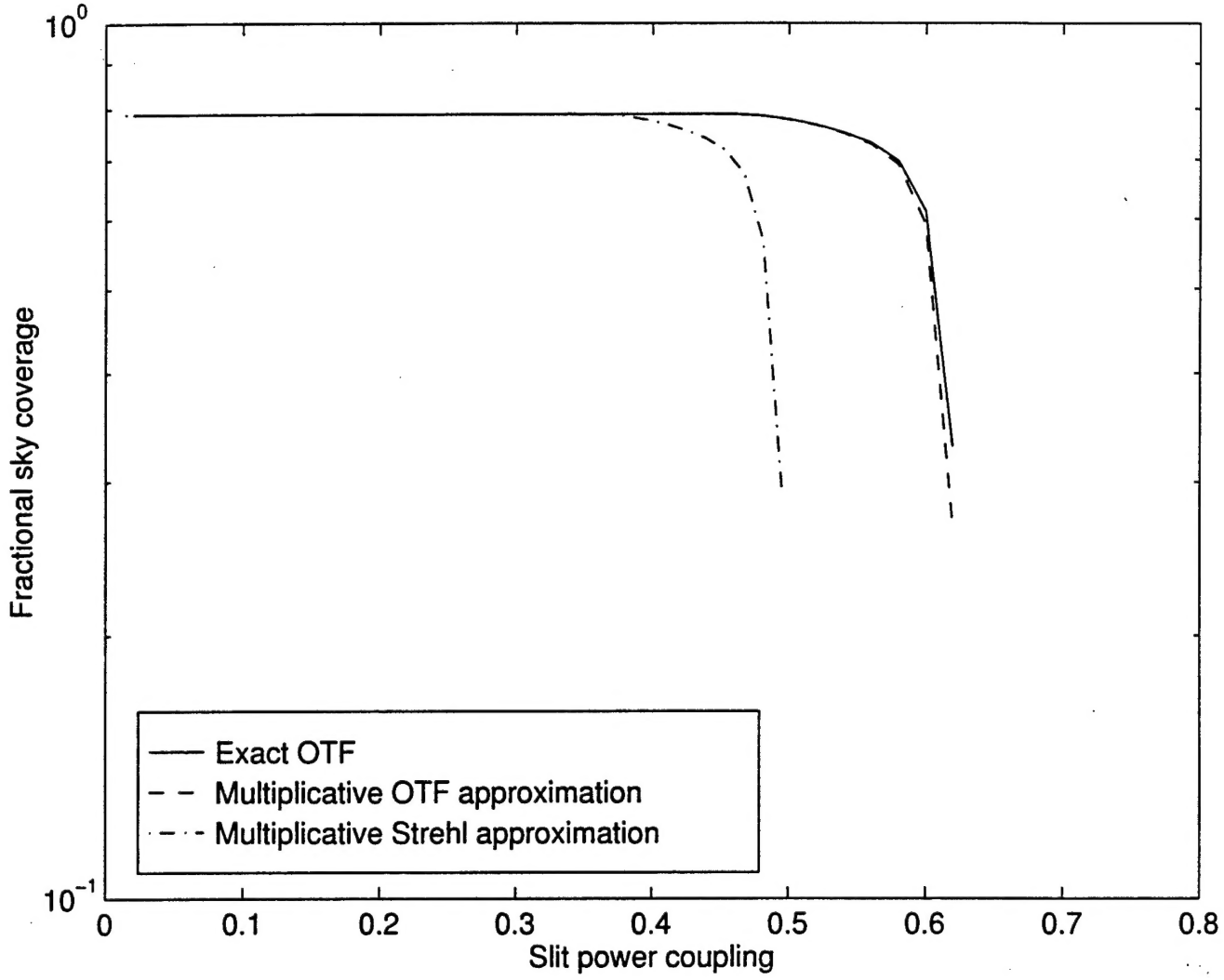
10^0
10^{-1}
Fractional sky coverage
0
0.1
0.2
0.3
0.4
0.5
0.6
0.7
0.8
Slit power coupling
Exact OTF
Multiplicative OTF approximation
Multiplicative Strehl approximation

Figure 13

Support for Starfire Optical Range

Schafer Corporation

2000 Randolph Rd., SE, Ste. 205

Albuquerque, New Mexico 87106

The work described in this document was accomplished by Mr David Tyler in collaboration with Dr Brent Ellerbroek of the Air Force Research Laboratory (AFRL) Starfire Optical Range. Dr Ellerbroek funded Schafer using a continuing Air Force Office of Scientific Research (AFOSR) grant. The grant supports an AFRL collaboration with the Gemini Telescopes Project (*http : //www.gemini.edu*) to develop and analyze adaptive optics (AO) methods. instrumentation, and performance for the Gemini-North telescope on Mauna Kea on the island of Hawaii. The scope of Schafer's work includes theory and analysis, numerical analysis and code development, and documentation of results for journal publication. This report summarizes work accomplished between March 1998 and November 1998, when Mr Tyler left Schafer Corporation. Attached is a draft journal article detailing the work performed in this period; the acknowledgments contain a statement that Mr Tyler was employed by Schafer when the work was performed. The draft article has been anonymously reviewed by two referees, and all issues raised by the referees have been addressed in the attached version. Following is a brief summary of the work performed.

Summary: Modelling the combined effect of static and varying phase distortion on the performance of adaptive optical systems. Adaptive optics (AO) systems are now in use at several astronomical observatories throughout the world to compensate the distorting effect of the Earth's atmosphere. Science results from working AO systems at the William Herschel, ESO 3.6m, and Canada-France-Hawaii telescopes are encouraging enough that AO retrofits to such venerable instruments as the Hale 200 in. and Lick 120 in. telescopes are well under way. However, the primary mirror diameters of these telescopes range from 3 to 5 meters, in what is now called the "intermediate" range of telescope size. The newest telescopes such as the Kecks, Suburu, and the Gemini North and South are all substantially larger, and as a consequence, substantially more expensive. Further, AO compensation of turbulence effects at optical and near-infrared wavelengths becomes more difficult with increasing aperture size. To fully exploit these large telescopes, then, AO modelling and design must be done at a level of detail previously unnecessary.

The existing literature suggests that most adaptive performance analysis is partitioned into separate treatments of time-varying atmospheric aberrations and static (or quasi-static) aberrations in the telescope optics themselves. Overall system performance is typically estimated by multiplying the associated Strehl ratios or optical transfer functions (OTFs). For AO-compensated residual aberrations, this multiplicative approximation is not formally exact. Since both the costs and expectations for large, ground-based telescopes are so challenging, it is prudent to examine in detail the domain in which the multiplicative approximation is actually valid.

This summary, and the attached paper, describes such a study. In particular, the approximations

$$S_{(t,s)} \approx S_t S_s. \tag{1}$$

$$H(\kappa)_{(t,s)} \approx H(\kappa)_t H(\kappa)_s / H(\kappa)_{dl}. \tag{2}$$

and

$$T(\boldsymbol{\kappa})_{(t,s)} \approx T(\boldsymbol{\kappa})_t T(\boldsymbol{\kappa})_s / T(\boldsymbol{\kappa})_{dl} \tag{3}$$

were examined, where S is the Strehl ratio, $H(\boldsymbol{\kappa})$ is the OTF, and $T(\boldsymbol{\kappa})$ is the speckle transfer function (STF). The subscipts t and s indicate time-varying and static quantities, respectively. The above quantities were calculated using numerical methods and compared over a range of static aberrations and a variety of atmospheric phase aberrations.

For a reasonably robust sampling of residual atmospheric and static aberrations, the multiplicative approximation for the total Strehl ratio $S_{(t,s)}$ is remarkably good as long as that quantity is larger than about 0.1. At lower performance levels, the approximation can be used as a moderately conservative lower bound. Similar conclusions apply to approximating a total OTF as the product of two factors. For higher-order moments of the OTF such as the STF, the approximation begins to fail at somewhat higher Strehl ratios; however, reasonable accuracy can still be achieved if the static aberration power is distributed fairly evenly over a range of spatial frequencies.

The validity of these approximations simplifies the design and use of AO systems for large telescopes as follows: During system design, an overall system OTF may be specified by separate characterizations of the two error sources (static and dynamic). Also, when AO-compensated imagery is processed after detection (or "deconvolved") to improve resolution further, the total OTF can be approximated by data from the AO wavefront sensor (see Ref. 3 in the attached paper) and an optical system OTF as calibrated by a local reference source.